SYNTHESIS AND CHARACTERIZATION OF CELL-RESPONSIVE BIODEGRADABLE POLYUREAS FOR LIGAMENT TISSUE ENGINEERING

A Thesis

by

NICHOLAS ALLEN SEARS

Submitted to the Office of Graduate and Professional Studies of
Texas A&M University
in partial fulfillment of the requirements for the degree of

MASTER OF SCIENCE

Chair of Committee,	Elizabeth Cosgriff-Hernandez
Committee Members,	Melissa Grunlan
	Jodie Lutkenhaus
Head of Department,	Gerard L. Cote

May 2014

Major Subject: Biomedical Engineering

ABSTRACT

The anterior cruciate ligament (ACL) is the most frequently ruptured ligament, accounting for an estimated 200,000 injuries and approximately 100,000 reconstructive surgeries each year in the United States. Due to the poor regenerative potential of the ACL and limitations of current ACL reconstruction techniques, development of a tissue engineered graft could have a significant clinical impact. Despite the robust and versatile properties of synthetic scaffolds, current iterations still have high failure rates due to degradation, wear, or fatigue. Polyurethanes utilizing ester-based soft segments were recently investigated as potential ligament grafts due to their established biocompatibility, excellent mechanical properties, and exceptionally tunable structure. However, non-specific hydrolytic degradation makes it difficult to match tissue regeneration, resulting in premature graft failure or stress shielding of the neotissue. In contrast, a biomaterial that features system-responsive degradation would integrate with native ligament remodeling and thus provide effective load transfer. It is well established that a graded load transfer from the graft to the neotissue during remodeling is necessary for proper organization of connective tissues which is strongly correlated to the resulting mechanical properties.

In this study, synthetic routes were first developed to create a linear polyurea elastomer system with appropriate chemistry to readily incorporate a biodegradable peptide diamine. Polyureas were selected due to their tunable segmental chemistry, high elasticity and fatigue strength, and mild reaction conditions that permits incorporation of

biological molecules at ambient conditions. Collagen-mimetic soft segments were first created by conjugating an enzyme-labile peptide diamine and commercially available polyether diamines. Candidate prepolymers were then chain extended with hexamethylene diisocyanate and mixed diamines. Particular focus was given to identifying compositions that permitted high molecular weight generation without gelation. By varying soft segment chemistry, soft segment molecular weight, and the hard-to-soft segment ratio, a library of polyureas was developed. This library was then used to elucidate key structure-property relationships necessary to tune mechanical properties and degradation rates of candidate polyureas. Finally, the enzyme-mediated degradation of candidate polyureas with variable peptide concentrations was investigated. In summary, synthesis of a novel biomaterial that combines the strength and tunability of synthetic elastomers with cell-responsive degradation will assist in the development of an improved tissue engineered graft for ACL reconstruction.

TABLE OF CONTENTS

Page

LIST OF FIGURES

Page

LIST OF TABLES

CHAPTER I

INTRODUCTION

1.1 Overview

Physical activity requires the cooperation of numerous specialized musculoskeletal tissues including muscle, bone, ligament, and tendon. Musculoskeletal tissue injury and disease can have an enormous impact on quality of life and results in billions of dollars in medical costs. The anterior cruciate ligament (ACL) is the most commonly ruptured ligament with over 200,000 injuries and 100,000 surgeries every year. Direct medical costs from surgical repair are estimated to be over five billion dollars.[1-3]

The ACL is the major intra-articular ligament of the knee that connects the posterior-lateral part of the femur to the anterior-medial part of the tibia. It provides necessary joint stability and prevents excessive anterior translation of the femur that could result in dislocation, bone fracture, or cartilage damage.[4] Damage to the ACL can result in pain, loss of mobility, joint instability, and often leads to injury of other tissues and the development of degenerative joint diseases, such as osteoarthritis.[5,6] After rupture, angiogenesis does not occur within the ACL for approximately 12 weeks.[7] As a result, damaged ACL tissue lacks significant vasculature and must depend on synovial fluid, contained within the joint capsule, for nutrient and waste transport. This inhibits natural regeneration and the result is often the need for surgical intervention.[5,8,9] The intrinsic properties of ACL-derived cells also play a role in its inadequate healing capacity.[10-14] ACL fibroblasts exhibit inferior proliferation, migration, and responses to

growth factors than fibroblast derived from the medial collateral ligament (MCL), and in response to injury, as well as demonstrate limited growth factor expression and lower upregulation of collagen type III, which has been shown to facilitate scar tissue formation.[10-15] Despite the large number of ligament reconstructions performed each year, an ideal grafting material has yet to be developed.[5,9] Current available reconstruction techniques for ACL repair include transplantation of autologous grafts, allogeneic grafts, and synthetic grafts.[2,16]

1.2 Current Ligament Reconstruction

1.2.1 Autografts

Despite inherent limitations, the use of tendon autografts has been recognized as the "gold standard" of ACL repair.[17-19] Autografts are typically harvested from the inner third of the patellar tendon or hamstring tendons and provide good mechanical strength as well as promote cell proliferation and differentiation[19-22]

The bone-patellar-bone graft incorporates bony blocks from the harvest site that allow for rigid fixation and reduce the chance of tendon creep[21,23,24] However, a large donor site incision and morbidity can lead to further complications such as harvest site pain, tendonitis, muscle atrophy.[24] The hamstring tendon graft has gained popularity over recent years due to reduced donor site morbidity and smaller incision size compared to patellar tendon grafts. The hamstring graft is harvested by removing the semitendinosus and gracilis tendons that are then folded in half and combined to make a quadruple-strand tendon graft.

The hamstring graft is a more comparable with the native intact ACL and the multiple strand graft may act as an analog to the two-bundle structure of the native ACL. Disadvantages of the hamstring tendon graft include donor site morbidity, tendon creep, and slow tendon healing due to the lack of a rigid fixation system. [22,25] The quadriceps tendon is less commonly used but allows for a larger fibrous portion that has the potential to increase mechanical properties. A bony plug for rigid fixation at one end also provides a potential for greater mechanical properties but size and location of the donor site scar along with donor site morbidity pose as serious disadvantages.[26] With all autografts, the donor site morbidity and limited availability are areas of concern that have given rise into investigation for a more suitable replacement.[26,27] During reconstructive surgery, the surgeon harvests a portion of the patient's patellar, hamstring, or quadriceps tendon to serve as a replacement ligament.[28,29]

A graft taken from the patellar tendon typically utilizes the middle third of the tendon, and is explanted with a piece of bone from the patella. This is combined with another piece of bone from the insertion point at the tibia.[4] A hole is then drilled through the tibia, where this "bone-patellar-bone" graft is inserted, stretched across the knee, and attached through another hole drilled into the femur. The "bone-patellar-bone" graft has high initial graft strength, and because it has a bone plug on each end, it can incorporate quickly with either fixation site. This allows for earlier motion of the knee and a shorter period of rehabilitation.[30]

In general, autografts typically possess good initial mechanical strength and promote cell proliferation, and they are conducive to graft remodeling and integration

into the joint.[19,30-32] Despite these advantages, the use of autogenous grafts is limited. Their long-term success is dependent on revascularization of the transplanted tissue, which is progressively surrounded by the synovial membrane.[7,33] The availability of autogenous grafts can be an issue, whether due to the need for multiple surgeries or age.[29,34] Finally, donor site pain, muscle atrophy, and tendonitis can lead to prolonged rehabilitation periods and can restrict patients from achieving pre-injury levels of activity.[35]

1.2.2 Allografts

Allografts typically use tendon grafts that have been harvested from cadavers and sterilized.[25] The use of allografts eliminates the need for a second surgical site and donor site morbidity.[22] Typical grafts are taken from the bone-patellar tendon or the Achilles tendon.[36,37] Allografts are more readily available than autografts and are incorporated into the body much like autografts but at a slower rate.[22] Disease transmission and bacterial infection have been a concern with the use of allografts. The chance of disease transmission from allografts is limited by harvesting grafts in sterile conditions, the use of a sterilization agent, and freezing the grafts until use.[22,38] However, sterilization methods such as ethylene oxide and gamma radiation can negatively impact the mechanical properties of the graft. [38] Ethylene oxide gas leaves behind the toxic residues ethylene glycol and ethylene chlorohydrins that cause synovitis and dissolution of the graft. Gamma radiation is used to eliminate bacteria and viruses from the donor tissue. Radiation levels between 1 and 2 Mrad eliminate bacterial threats but radiation levels on

the order of 4 Mrad radiation are required to eliminate viruses. However, above 3 Mrad has been to shown to alter the mechanical properties of the graft and change the tissue morphology.[22,36] Dry freezing and cryofreezing bypass the sterilization process and retain the grafts original mechanical properties.[39] However, the chance of disease transmission and bacterial infection remains of concern.

To circumvent problems associated with autogeneic tendon grafts, the use of allografts has been employed for ACL repair. Allografts are tissues harvested from a cadaver, such as the patellar, hamstring, and achilles tendon, which eliminates the need for an additional surgical site.[40,41] This reduces surgical time and minimizes postoperative pain.[34] Like autografts, allografts provide good initial mechanical strength and promote cell proliferation and remodeling, with the added benefit of an unlimited graft supply.[19,39] Nevertheless, there are still limitations to this therapy including disease transmission, bacterial infection, and unfavorable immunogenic responses.[18,42] Although sterilization and preservation can minimize these risks, they also reduce the tensile properties of the graft, limiting its use for ACL reconstruction.[17,34,36,43,44]

1.2.3 Synthetic Grafts

Due to the limitations of biologic grafts, synthetic materials have been investigated for potential use in ACL reconstruction.[45,46] These grafts do not require sacrifice of autogenous tissue and do not lose their strength due to tissue remodeling, which allows for much faster rehabilitation.[47] Prostheses of homogenous, non-degradable polymers evaluated for ACL repair include carbon fiber, the Gore-Tex

ligament (polytetrafluoroethylene), the Stryker-Dacron and Leeds-Keio ligaments (polyethylene terephthalate), and the Kennedy Ligament Augmentation Device (polypropylene).[5,9,18,33,46,48-50] The Gore-Tex ligament is composed of a single, continuous fiber of expanded polytetrafluoroethylene (ePTFE) that is wound into multiple loops and joined together to form a braid.[51] The Stryker-Dacron ligament consists of a core of four tightly woven Dacron tapes encased by a sleeve of loosely woven Dacron velour, and it was designed to promote tissue ingrowth.[41,52] Similar to the Stryker-Dacron ligament, the Leeds-Keio ligament is composed of polyethylene terephthalate (PET) with an open-weave tube to promote ingrowth of fibrous tissue.[53,54] Finally, the Kennedy Ligament Augmentation Device (LAD) is a cylindrical prosthesis with a diamond-braided construction, and it was designed for simultaneous implantation with a biologic graft to augment the tissue and protect it during the early stages of healing.[55,56] The Gore-Tex and Stryker-Dacron ligaments have each received general release from the Food and Drug Administration (FDA) as permanent ligament replacements, but only to salvage previously failed intra-articular reconstructions.[34,54]

Although these devices typically provide immediate stabilization of the joint, they are unable to duplicate the mechanical behavior of the ACL and eventually fail due to material fatigue.[9,34] Due to the high linear stiffness of synthetic implants, a majority of the physiological load is borne by the prosthesis, effectively stress shielding the surrounding tissue.[4,9,57,58] Without proper mechanical cues to direct collagen alignment and tissue organization, the load-bearing capacity of the native tissue is reduced so that the synthetic graft is limited to its inherent fatigue properties. In addition to graft

rupture, repeated elongation of these devices can lead to permanent deformation at points of stress, which results in a loosening of the ligament and a loss of joint stabilization.[59,60] Contact with sharp edges of the bone tunnels can also cause abrasions that weaken the implant and create debris, which can elicit an unfavorable foreign body response.[9,61] Woven prostheses face additional challenges such as axial splitting, low extensibility, low tissue infiltration, and abrasive wear that can lead to synovitis in the joint.[4,5,9,57,58,62] Long-term studies have also revealed a high incidence of osteoarthritis post implantation.[60,63] Overall, the limitations of current ACL reconstruction strategies present a substantial margin for improvement in the escalating market for ACL repair.

1.3 Anterior Cruciate Ligament Tissue Engineering

Musculoskeletal tissue engineering has received growing interest throughout orthopedic medicine as a promising alternative to biologic and synthetic grafts.[4,33,64,65] Tissue engineers attempt to harness the body's natural ability to repair and regenerate damaged tissue through the application of biological, chemical, and engineering principles. This strategy can potentially improve upon current clinical options by providing appropriate biological and mechanical properties to regenerate damaged ACL tissue without the aforementioned limitations of other grafts.[4,5,9,66] ACL reconstruction utilizing a tissue-engineered ligament would eliminate donor site pain and morbidity, improve and accelerate rehabilitation, provide a limitless supply of graft tissue, eliminate the risk of disease transmission or unfavorable immunogenic responses, and increase the fatigue life of the graft.[5,9]

The traditional tissue engineering paradigm combines isolated cells and bioactive factors on a biodegradable scaffold that is able to sustain functionality during tissue regeneration. The scaffold serves as a structural template to enhance neotissue formation and structure, **Figure 1.1**.[5,9,66,67] In ligament constructs, scaffolds are seeded with fibroblasts or mesenchymal stem cells that are then provided with the necessary mechanical and biochemical cues to initiate ligament regeneration. To facilitate this process, the biomaterial selected for these constructs must be biocompatible, biodegradable, and permit typical cell-material interactions necessary for cell proliferation, migration, and differentiation. The scaffold must also demonstrate interconnected porosity to enable nutrient transport, waste removal, and tissue infiltration. Finally, the tissue engineered construct must demonstrate appropriate mechanical behavior to maintain functionality throughout native tissue remodeling. The need to duplicate the complex function and unique mechanical properties of the ACL at all stages of remodeling is partly responsible for the difficulty encountered in developing a suitable surgical replacement. Therefore, advancement of ligament tissue engineering strategies is strongly dependent on the ability of tissue engineers to develop a biomaterial scaffold that reproduces both the mechanical and physiologic properties of native ACL tissue.

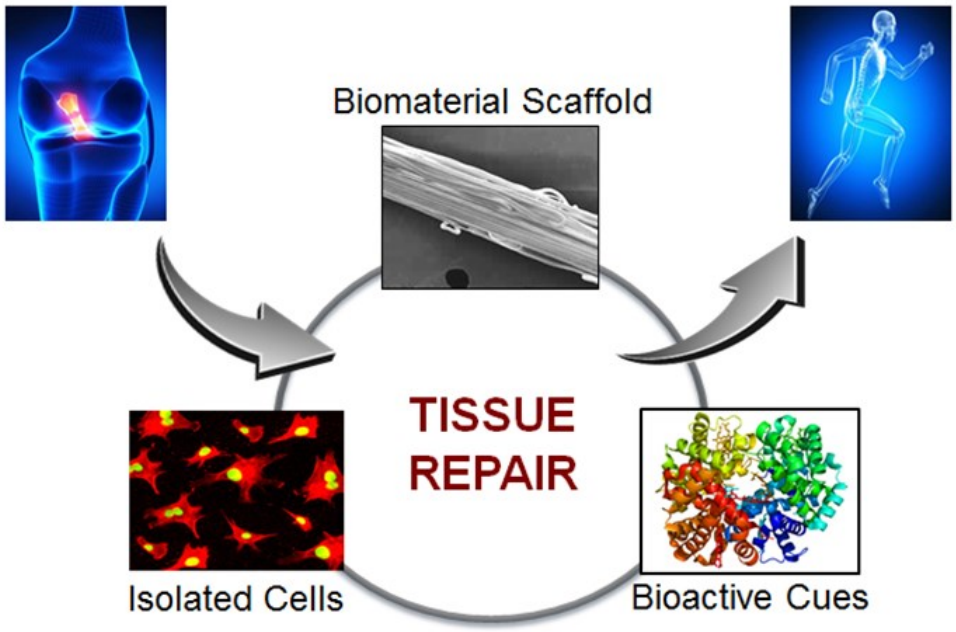

Figure 1.1. Tissue engineering paradigm.

Knowledge of ligament structure and its components is extremely important in the development of a scaffold for ligament tissue engineering. Interactions among such components and their arrangement in the tissue give ligaments their unique mechanical properties.[4] The ACL is predominantly composed of collagen, elastin, proteoglycans, glycoproteins, water, and fibroblasts.[4,68] Fibroblasts not only synthesize fibrillar collagen but also enzymatically break down and remove old collagen as part of native tissue remodeling. Collagen account for almost 80% of all protein synthesis in the ACL. Type I and type III collagen comprise approximately 88% and 12%, respectively.[69,70] Type I collagen forms tough, nonelastic cross-linked fibers that contribute to the tensile strength of ligaments and tendons.[68,70] Type III collagen forms loosely organized, thin fibrils that

provide elasticity.[68,70] Type I collagen molecules form a hierarchical structure of dense, highly organized, cable-like tissue in which fiber bundles orient parallel to the longitudinal axis in a helical formation.[4,5,9,69,71] Fibroblasts align between these collagen bundles and elongate in the direction of loading.[69] Fiber bundles form a periodic crimp pattern that permits 7 to 16% creep before permanent deformation or ligament damage can occur. Overall, it is this complex, hierarchical structure that dictates the bulk tensile properties of the ACL.

The mechanical and viscoelastic properties of the human ACL have been well-documented. The human ACL is regularly exposed to cyclic loads as high as 630 N through all degrees of knee joint flexion/extension.[72] Its ultimate tensile strength of was found to be 1730 N, with a linear stiffness of 182 N/mm and 12.8 N-m for energy absorbed at failure, although such properties have been found to increase during development and diminish with age.[73-75] The maximum strain that a ligament can endure before failure is between 12 and 15%.[76] When exposed to strain, the ACL demonstrates triphasic behavior, starting with a non-linear, toe region where the ligament exhibits low amount of stress per unit strain.[4] This results from a lateral contraction of fibrils, the release of water, and straightening of the crimp pattern. Once the crimp pattern has fully straightened, force is directly applied to the collagen triple helix and interfibrillar slippage occurs between crosslinks, forming a linear region in which stress increases per unit strain.[77-79] Eventually, collagen fibers begin to defibrillate, leading to a slight decrease in stress per unit strain and failure.[4,77,80] A biomaterial scaffold that can

replicate this mechanical behavior and integrate with the native tissue is necessary for the development of a successful tissue engineered ligament, **Figure 1.2.**

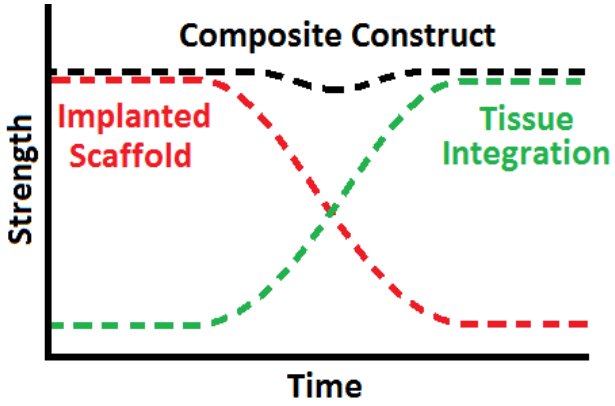

Figure 1.2.Stress-strain behavior of graft-tissue composite throughout the remodeling process.

1.4 Current Biomaterial Scaffolds for Ligament Tissue Engineering

1.4.1 Natural Polymer Grafts

Biocompatible and degradable biomaterials that have been investigated for ligament tissue engineering include natural polymers, such as collagen and silk, and synthetic materials. Type I collagen was selected as a biomaterial scaffold due to its abundance in ligament tissue and its ability to support the growth of fibrous tissue. Examples of tissue-engineered approaches using collagen fibers are presented extensively throughout the literature.[81,82] Dunn et al. constructed fibroblast-seeded scaffolds composed of type I collagen fibers and found that such devices remain viable after implantation, showing excellent biocompatibility, enhanced cell attachment,

proliferation, and extracellular matrix production.[82,83] Nevertheless, these scaffolds are unable to maintain the mechanical integrity necessary to restore ligament function. Several strategies have been attempted to enhance the mechanical properties of collagen-derived scaffolds, including cross-linking and copolymerization/blending with synthetic polymers.[9,34,84-90]. Despite these efforts, relatively quick in vivo degradation and the resulting loss of mechanical strength are still major concerns with using collagen fibers for ligament tissue engineering.[81,91] High cost, variability, complex handling properties, and potential disease transmission further limit the use of collagen, prompting the search for an improved biomaterial.[34,92]

Due to its high tensile strength and linear stiffness, biocompatibility, and biodegradability, silk has received renewed interest as a potential biomaterial for tissue engineering.[93-97] The excellent mechanical properties of silk result from the high homogeneity of its secondary structure (β-sheet), extensive hydrogen bonding, and crystallinity. Silk is composed of a fibroin core and a glue-like sericin cover, and although sericin in silk has been shown to cause adverse problems with biocompatibility, there are several methods to remove it before usage. As a result, scaffolds constructed of silk fibroin demonstrate good biocompatibility and have been shown to support cell adhesion.[98] In addition, by coating the surface of these scaffolds with RGD sequences, increased cellular attachment, proliferation, and extracellular matrix production have been observed.[99] When organized into an appropriate wire-rope geometry, silk fibroin exhibits mechanical properties similar to the native ACL.[98] For example, Altman et al. constructed a tissue-engineered device consisting of a twisted

fibrous matrix composed of silk fibers arranged into a hierarchical structure similar to the native ACL. Through modification of scaffold architecture, the stiffness of the scaffold can also be decreased to prevent stress shielding while maintaining tensile strength. Silk undergoes proteolytic degradation at a rate that is dependent on its environment, but typically silk fibers lose their tensile strength within one year in vivo and degrade completely within two years. The slow rate of silk degradation allows for gradual load transfer from the polymer scaffold to newly formed tissue.[35] Even though silk has demonstrated much promise for ligament tissue engineering, its dependence on scaffold architecture to achieve mechanical properties limits independent control of mechanical strength and degradation necessary to promote effective load transfer.

Along with collagen and silk, other natural polymers have been investigated for potential use in ACL reconstructions. Funakoshi et al. constructed a tissue engineered scaffold from novel, chitosan-based hyaluronan hybrid polymer fibers, which were shown to exhibit enhanced mechanical properties and biological effects in vitro.[100] Majima et al. investigated the effect of alginate-based chitosan hybrid polymers on fibroblast adhesion, extracellular matrix synthesis, and mechanical properties.[100] Finally, Messenger et al. investigated the ability of enamel matrix derivative to enhance tissue induction around scaffolds used in ACL reconstruction.[101] These studies have considerable potential for ligament tissue engineering; however, they are still in preliminary stages of development and are far removed from clinical applications. Overall, despite the aforementioned advantages of natural polymers, major concerns stem from issues with mass production, variability, and the lack of independent control

of degradation rate and mechanical properties, which limits their usefulness for ACL repair.

1.4.2 Synthetic Polymers Grafts

In addition to natural polymers, biodegradable, synthetic polymers have been investigated for ACL repair, including poly (glycolic acid) (PGA), poly (L-lactic acid) (PLLA), poly (lactic-co-glycolic acid) (PLGA), polydioxanone (PDS), and poly (desamino-tyrosyl-tyrosine ethyl carbonate) (poly (DTE carbonate)).[4,66,102-108] Similar to nondegradable synthetic polymers used to construct permanent prosthesis, there is no limit to graft supply and no risk of disease transmission. Unlike natural polymers, such as silk, which rely on modification of scaffold architecture to alter mechanical properties, the performance properties of synthetic polymers can also be controlled with polymer chemistry. For instance, the mechanical properties of a device may be controlled by altering the degree of polymer crystallinity or changing its molecular weight.

PGA and PLLA are excellent candidates for ligament tissue engineering because they are biocompatible, do not elicit unfavorable foreign body responses, and naturally degrade into non-toxic byproducts (glycolic acid, lactic acid). Additionally, because tissue engineered scaffolds are eventually replaced with neotissue, the fatigue properties of PGA and PLLA are not a concern. As a result, PGA, PLLA, and PLGA have been extensively studied for potential use in ACL reconstruction. [4,66,104-108] In particular, Laurencin et al. developed a series of cell-seeded, three-dimensional scaffolds from

PGA, PLLA, and PLGA using a novel braiding technique designed to enhance mechanical properties and promote tissue infiltration, with PLLA proving to be the best option for ACL repair.[37,109] Similar to native ligament tissue, these braided scaffolds have a hierarchical structure composed of fibers arranged into bundles and wound throughout the thickness of the scaffold. This braiding technique was developed to create scaffolds with controlled pore size, integrated pores, resistance to wear and rupture, and mechanical properties comparable to the ACL. In in vitro studies, ACL fibroblasts were found to conform to the geometry of the scaffolds, exhibit spindle-like morphologies, and demonstrate extracellular matrix production. Additionally, cellular proliferation, tissue growth, and long-term extracellular matrix production were enhanced in the presence of fibronectin, an adhesion protein found in the extracellular matrix of native ligament tissue. These results suggest that braided scaffolds constructed of PLLA may become a viable option for ACL repair.[37,109,110]

Other synthetic polymers explored for potential use in ligament tissue engineering include PDS and poly (DTE carbonate). Buma et al. studied autogenous reconstruction of the ACL in goats in the presence of a degradable augmentation device composed of PDS and found that, after 6 weeks, a rapid decrease in strength was observed for augmented transplants.[103] In contrast, non-augmented transplants demonstrated a gradual increase in strength. These results suggest that PDS is a poor choice for ligament tissue engineering due to its rapid degradation. Bourke et al. fabricated ACL scaffolds from poly (DTE carbonate) fibers and found that these scaffolds have mechanical properties similar to the native ACL, and that they keep a

much higher ultimate tensile strength (87% of original) after 30 weeks of degradation than PLLA (7% of original).[102] Despite these advantages, the parallel arrangement of poly (DTE carbonate) fibers in these scaffolds leaves them susceptible to long-term failure due to fatigue and creep.

Overall, current research has shown that synthetic, biodegradable polymers can be viable options for ACL reconstruction; however, these materials are still limited in their ability to serve as ligament replacements. This is because the majority of these polymers lack the inherent material properties necessary to restore the mechanical strength and elasticity of the ACL. To overcome these mechanical limitations, a number of scaffolds derive their properties from their geometry and method of fabrication; however, this requires an understanding of how each structure behaves mechanically relative to one another. Changes in the mechanics of scaffold architecture due to degradation or repeated loading then increase the complexity of the graft, making it difficult to optimize scaffold design to promote effective load transfer. In addition to scaffold fabrication, polymer chemistry can be tailored to modulate these performance properties; however, a number of these structure-property relationships have overlapping components that complicate material design. For example, it is widely accepted that polymer crystallinity can be used to predict polymer modulus, yet highly crystalline polymers have also been shown to demonstrate slower hydrolytic degradation than amorphous polymers.[111] Without mechanisms to isolate specific structure-property relationships, these polymers are unable to balance the dual impact of tensile properties and the rate of degradation on the regeneration of ligament tissue. Additionally, the

degradation mechanism for the majority of these polymers is non-specific hydrolysis, which makes it difficult to tailor scaffold degradation to complement neotissue formation. An improved material is needed to develop a successful tissue engineered ligament, because synthetic polymers are typically unable to either match the mechanical behavior of the ACL or integrate with native tissue remodeling.

1.5 Segmented Polyurethane Elastomers

Due to the aforementioned limitations of current synthetic polymers, polyurethane elastomers have received growing interest for ligament tissue engineering.[112-115] Polyurethanes were first developed by Otto Bayer of I. G. Farbenindustrie, Leverkusen, Germany, in 1937.[112] Since then, polyurethanes have been used in a wide range of industrial applications, including machinery, textiles, packaging, adhesives, and sealants.[116,117] Because of their outstanding mechanical properties and established biocompatibility, polyurethanes have also been used in a variety of biomedical applications over the past 40 years.[112,118-120] Polyurethane chemistry dictates the physical, biological, and mechanical properties of these polymers and can be tailored to provide a variety of materials, such as soft elastomers, rigid thermosets, and foams.[112,116,117,121] Therefore, understanding the hierarchical structure of polyurethanes and related materials, along with relevant structure-property relationships, is essential for effective biomaterial design.

Polyurethanes are a class of polymers that consist of urethane (-NH-CO-O-) linkages, typically generated by the reaction of isocyanates with hydroxyl-functional

molecules by addition to the carbon-nitrogen bond.[121-123] Similarly, polyureas contain urea linkages (-NH-CO-NH-) and are generated by the addition of isocyanates and primary amine groups. Polyurethane and polyurea elastomers used for biomedical applications are typically linear, alternating block copolymers that consist of comparatively high molecular weight soft segments linked with urethane/urea containing hard segments.[112-114] Common soft segments include hydroxyl-terminated polyethers, polyesters, and polycarbonates, all of which have relatively low glass transition temperatures. In contrast, hard segments usually have high glass transition temperatures and are characterized by semicrystalline, aromatic or aliphatic diisocyanates linked with a low molecular weight chain extender.[112] Thermodynamic incompatibility between these segments drives microphase separation in which hard segments form glassy, semicrystalline domains that, in polymers of lower hard segment content, are dispersed within an amorphous, rubbery matrix.[112-114,124,125] These hard domains are stabilized by hydrogen bonds formed between urea and urethane linkages which then serve as physical crosslinks and retain and reinforce the soft segment matrix.[112,124,125] It is this microphase-separated morphology that dictates the ease of processing of polyurethane elastomers. This is because, unlike traditional elastomers which derive their elasticity from an amorphous network interconnected with chemical crosslinks, the physical crosslinks of polyurethane elastomers are thermo-reversible and so breakup upon heating or dissolution.

Along with this ease of processing, the mechanical properties of segmented block copolymers are strongly dependent on this microphase-separated morphology.

Deformation of segmented block copolymers begins with elastomeric stretching of the soft segment matrix, as indicated by a low initial modulus in the stress-strain curve, **Figure 1.3**.[126] Hard domains then breakup at flaws and begin to rotate into the strain direction, causing a plateau of almost constant stress. This eventually results in the formation of microfibrils consisting of small, semi-crystalline hard domains separated by strain-crystallized soft segment chains that undergo strain hardening at higher strains.[126] Ultimately, these hard domains shear yield at a critical strain and the material fails.[126]. Because of this deformation profile, polyurethanes and polyureas have excellent mechanical properties, including high tensile strength, elongation to failure, fatigue life, and wear resistance, without additional processing. In addition to mechanical behavior, microphase separation has also been shown to directly influence the rate and extent of biodegradation.[127,128] Factors that influence the degree of phase separation include soft segment molecular weight, hard and soft segment chemistries, and the hard to soft segment ratio.[129-133] Therefore, these variables can be adjusted to modulate the performance properties of polyurethanes and polyureas. For example, increased hard segment content puts greater constraint on the soft segment matrix, which leads to a higher initial modulus and strain hardening at a lower strain.[126,134]

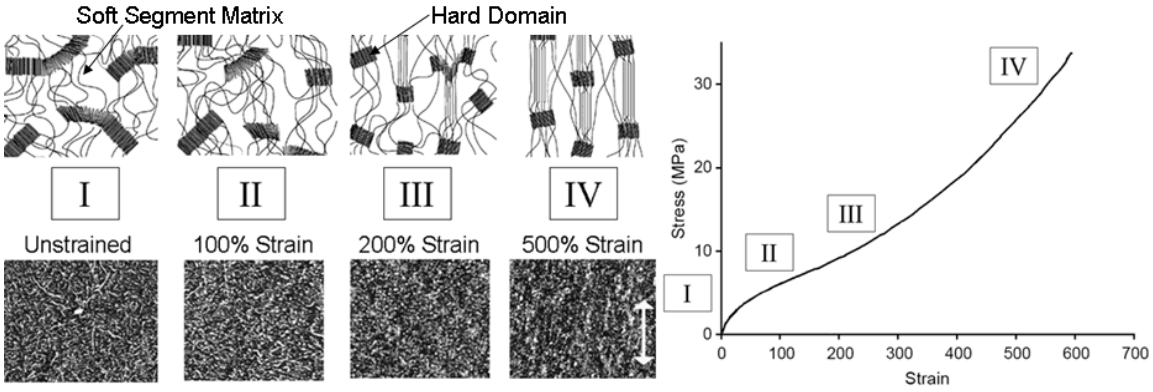

Figure 1.3. Effect of mechanical stretch on polyurethane deformation. Reprinted with permission from "Relationship between nanoscale deformation processes and elastic behavior of polyurethane elastomers", by Christenson, EM, Anderson, JM, Hiltner, A, Baer, E, Polymer, 46(25):11744-11754, Copyright 2005 by Elsevier.[126]

Overall, the correlation between polyurethane chemistry and microphase separation, and thus performance properties, provides a means to elucidate key structure-property relationships. As with homogenous, biodegradable polymers, a number of these relationships have overlapping components that complicate material design for tissue engineering applications. A key challenge then is to isolate structure-property relationships that are essential to the development of engineered tissue. A polymer system with several mechanisms to modulate physical properties would provide the tools necessary to observe such phenomena. Due to the exceptional tunability of polyurethanes and polyureas, segmental modification of these polymers can be used to generate a library of polymers with broad structural diversity and a myriad of performance properties to better probe specific tissue-biomaterial interactions. Greater

understanding of such structure-property relationships would then allow for rational design of a tissue engineered scaffold that promotes effective load transfer.

1.6 Biodegradable Polyurethane Scaffolds

As stated previously, in addition to the aforementioned mechanical requirements, tissue engineered scaffolds must be biocompatible and biodegradable. Polyurethanes used for biomedical applications have traditionally been intended for biostable, long-term use, such as cardiovascular applications and artificial organs.[112,120] Aromatic diisocyanates were often chosen for these materials due to their enhanced mechanical properties; however, concerns that the degradation of these diisocyanates (i.e., 4,4'-methylenediphenyl diisocyanate (MDI), 2,4-toluene diisocyanate (TDI)) can generate potentially carcinogenic byproducts (i.e., 4,4'-methylenedianiline (MDA), 2,4-toluene diamine (TDA)) have limited their transition to biodegradable polymers.[115,135-137] As a result, aliphatic diisocyanates, such as hexamethylene diisocyanate (HDI) and L-lysine diisocyanate (LDI), have received interest for tissue engineering.[132,138-149] Unlike aromatic diisocyanates, polyurethanes prepared from aliphatic diisocyanates have been reported to degrade to non-cytotoxic compounds in vitro and in vivo.[150,151] LDI and HDI-based biodegradable polyurethanes have also demonstrated excellent mechanical properties and good biocompatibility, as well as promoted cell-material interactions necessary for tissue formation.[152-154] In addition to biocompatible diisocyanates, biodegradable hard segments composed of enzyme-labile chain extenders have been used to synthesize polyurethanes for tissue engineering.[142,151,155] Degradation of these

linkages is dependent on hard segment crystallinity; however, crystallinity is a well-established barrier to degradation. Additionally, enhanced hard segment crystallinity leads to an increase in supramolecular interactions (i.e., hydrogen bonding) that dictate the mechanical properties of polyurethane elastomers. Due to the interactions among crystallinity, degradation rate, and mechanical strength, biodegradable hard segments limit the inherent tunability of polyurethane elastomers by inhibiting independent control of these structure-property relationships.

In contrast, the use of biodegradable soft segments can potentially decouple the effects on polyurethane structure on degradation rate and mechanical properties. Polyurethanes have been synthesized from a number of biodegradable soft segments, including poly (lactic acid), poly (glycolic acid), and poly (ε-caprolactone) (PCL).[139-143,149,156-162] These polyols were selected based on their established hydrolytic degradation in vitro and in vivo. As a result, polyurethane degradation is dependent on soft segment content, chemistry, and molecular weight. Several polyurethanes composed of these polyols have demonstrated biocompatibility and excellent mechanical properties, as well as promoted tissue remodeling.[151,159] Indeed, Gisselfalt et al. developed a series of PCL-based poly(urethane urea) fibers for ligament tissue engineering that displayed high tensile strength, modulus, and fatigue resistance, as well as supported ingrowth of connective tissue.[134,163] Nonetheless, as with biodegradable polyesters previously used for ligament tissue engineering, degradation of these soft segments is dictated by non-specific hydrolysis, which makes it difficult to tailor polyurethane degradation to complement tissue regeneration.

However, the semi-crystalline nature of some of these soft segments can impact the performance properties of these materials. For example, PCL of higher molecular weight can lead to increased crystallinity of the soft segment, and thus a corollary increase in the modulus and tensile strength, along with a decreased rate of degradation.[132,142] Therefore, soft segment crystallinity further compounds the complexity of polyurethane morphology and derived properties, which makes independent control of polyurethane structure-property relationships through segmental modifications difficult. In order to disrupt the crystallinity of PCL and increase the range of degradation rates, PCL and poly (ethylene glycol) (PEG) copolymers have been investigated; however, the hydrophilicity of PEG increases water uptake, which increases the rate of degradation.[150,156,159,164-166] Overall, although segmented block copolymers possess the tools necessary to tailor biomaterial chemistry and thus provide independent control of degradation and mechanical properties, non-specific degradation of current polyurethane elastomers makes it difficult to complement scaffold degradation with ligament regeneration.

1.7 System-Responsive Degradation

In general, the design of biomaterial scaffolds for tissue engineering is currently limited by the ability of the scaffold to restore function throughout the life of the implant. The scaffold must provide initial mechanical stability and function, but must retain adequate strength and function while the scaffold degrades and neotissue is formed. The rate of degradation in polymers such as polyesters (which undergo non-specific degradation via hydrolysis) is dependent on the environment, which is heavily

dependent on the individual. Temperature, pH, and mechanical stresses can cause degradation to vary significantly, complicating design of a scaffold to fit a certain degradation profile. Due to this dependency on mechanical loading, a major challenge in the design of a successful tissue engineered ligament is to facilitate load transfer from the biodegradable scaffold to newly formed tissue. Initially, the biodegradable scaffold should exhibit sufficient mechanical properties to provide immediate mechanical stability and restoration of ligament function. Isolated cells should then generate neotissue at a rate complementary to scaffold degradation so that the mechanical integrity of the ligament is sustained throughout the remodeling process up until the injured tissue is completely replaced.[4,9,167] Because the level of load borne unto *de novo* tissue dictates remodeling and thus, collagen alignment, a degradation rate that does not match new tissue formation can lead to either graft rupture (too fast) or stress shielding (too slow).[4,66,98] With stress shielding, the lack of collagen alignment can shift the dynamics of ligament remodeling toward degradation, which reduces the load-bearing capacity of the newly formed tissue. In order to integrate with native ligament remodeling and maintain mechanical functionality, new structure-property models are needed to elucidate the mechanisms of load transfer. A polymeric system with control over degradation rate and mechanical properties would provide insight into these mechanisms and allow for rational design of tissue engineered constructs. Biodegradable polyurethanes can be tailored to isolate the effects of polymer structure on specific performance properties; however, utilizing non-specific degradation remains

problematic, given that these rates can vary based on the individual, environment, and circumstances.

Appropriate mechanical cues are required for neotissue to successfully form the hierarchical structure of ACL tissue. Independent control over mechanical properties and degradation would allow for tailoring of degradation to compliment neotissue formation, and prevent premature graft rupture. Current research has established that mechanical stimulation increases fibroblast proliferation. It has been shown that the extent of this effect is dependent on the type and magnitude of this loading, as well as the duration.[66,168-171] In addition, cyclic stretch has been shown to cause cells to adopt an elongated morphology consistent with the ligament phenotype.[168,172-175] Mechanical loading is also needed to induce cellular alignment via restructuring of the actin cytoskeleton.[172,176,177] The orientation of fibroblasts with respect to mechanical loading is of particular winterest because of its influence on *de novo* tissue formation.[173,178-181] Fibroblasts oriented parallel to the direction of stretch demonstrate greater protein synthesis than cells aligned perpendicular to the direction of stretch, as well as generate an oriented collagen matrix.[173,178] These effects have clear relevance to the mechanical properties of the resulting tissue. Finally, physical loading has been shown to increase protein synthesis, specifically type I collagen, which is of particular importance in the ACL due its role in establishing tensile properties.[168,172-174,177,182-184] Overall, these studies establish the need for mechanical stimulation to develop highly organized, cable-like tissue, indicative of the native ACL.

System-responsive degradation would circumvent this limitation by integrating polyurethane biodegradation with native ligament remodeling. As stated previously, during tissue regeneration, fibroblasts produce enzymes that systematically break down and remove the existing extra cellular matrix.[185] Specifically, matrix metalloproteinase (MMP) production, including MMP-1 and MMP-2, is upregulated due to a ligamnent injury such as a rupture and mechanical stimulation. Additionally, it has been demonstrated that MMP-2 is the most efficient enzyme associated with type I collagen degradation.[186-188] The specificity of these enzymes has been extensively investigated with cleavage localized to the (Gly_{775}-Ile_{776}) site of the triple-helical collagen.[189-191] By incorporating this collagen oligopeptide sequence into the design of a novel biomaterial, guided scaffold degradation can be achieved. Moreover, integration of this enzyme-labile peptide sequence into the soft segment of a polyurethane elastomer would provide a means to decouple degradation rate from other performance properties.

For this study, an enzyme-labile peptide sequence with established specificity to MMP-2 was conjugated to ether-based polyols to form collagen-mimetic soft segments, **Figure 1.4.** Synthetic routes were first developed that would allow for the chemical incorporation of a diamine functional peptide into a polymer backbone. Upon successful conjugation, biodegradable soft segments were used in the synthesis of linear polyurea elastomers. By varying soft segment chemistry, soft segment molecular weight, and the hard to soft segment ratio, a series of cell-responsive, biodegradable polyureas was developed to elucidate key structure-property relationships necessary to complement neotissue formation. Overall, a novel biomaterial that combines the strength and

tunability of synthetic elastomers with cell-responsive degradation will assist in the development of an improved tissue engineered graft for ACL reconstruction.

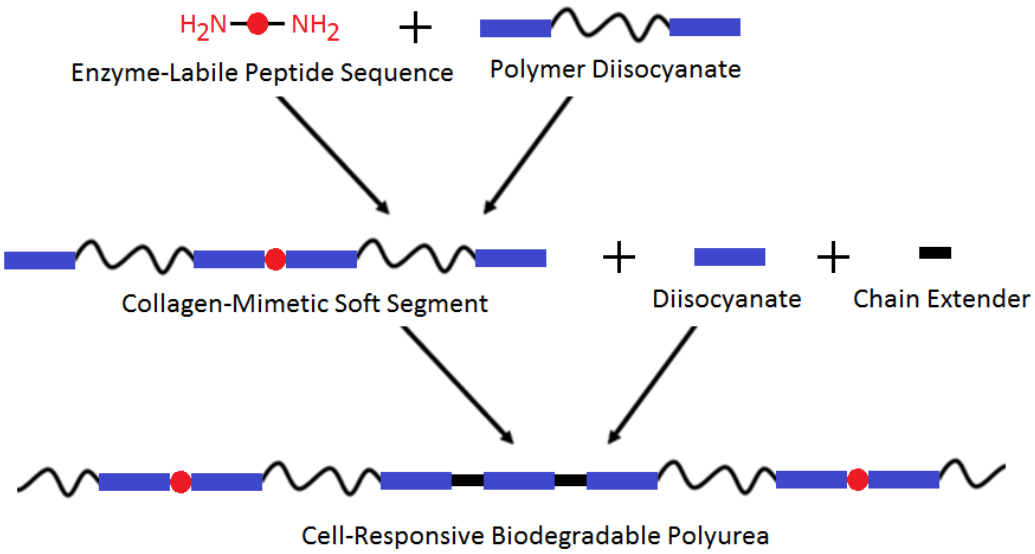

Figure 1.4. Synthetic design of cell-responsive, biodegradable polyureas.

CHAPTER II

MODEL BIOSTABLE POLYUREAS

2.1 Introduction

Polyureas are a class of segmented block copolymers that are similar to polyurethanes in many aspects. Urea linkages are formed by the reaction of isocyanates with amines, rather than hydroxyl groups. This reaction is much more energetically favorable, allowing for reaction at room temperature without catalyst[192,193]. Thermoplastic polyurea may be described as linear, alternating block copolymers consisting of comparatively high molecular weight soft segments linked with urea containing hard segments (HS).[112-114,194] Polyurea HS consist of diisocyanate molecules linked with short diamine chain extenders.[112] Changes in soft segment chemistry, soft segment molecular weight, HS chemistry, and HS content, among other factors, have been shown to affect the degree of phase separation and resulting mechanical properties.[129-133,195-199] This tunable segmental chemistry provides multiple avenues to modulate mechanical properties to meet specific design targets.

In addition to requirements of elasticity and fatigue resistance, review of the properties of the ACL and loading can be used to identify requisite strength of polyurea ligament grafts. The size and strength of the human ACL ranges widely depending on the individual's age and gender, and varies significant within these groups as well. One study reported an average cross sectional area of the middle portion of the ACL to be 60.1 mm ± 16.9 mm^2.[200] Another study found a peak walking load of 303 N.[201] This would then produce a tensile stress of 5.04 MPa. Criteria for a potential tissue

engineered ligament graft were established as an ultimate tensile strength of 10 MPa, approximately two times the average load while walking.

Hard segment content is one of the strongest predictors of strength in segmented polyureas with higher HS content yielding greater strength.[199] However, higher HS content is also associated with gelation during synthesis which can prevent high molecular weight formation and difficulty in processing. Gelation is a much more significant issue in polyureas due to the formation of "bidentate" hydrogen bonds in which both hydrogens within the urea linkage hydrogen bond with the two free electron pairs of an oxygen atom in a nearby carbonyl, **Figure 2.1**. These bidentate hydrogen bonds can become so strong that reaction solutions gel and become unprocessable even upon dilution, significant heat, and the addition of hydrogen bond disruptors. Alteration in chain extender chemistry including changes in HS registry, symmetry, and sterically-hindering groups have been used to prevent gelation and improve processability by limiting hydrogen bonding.[202,203]

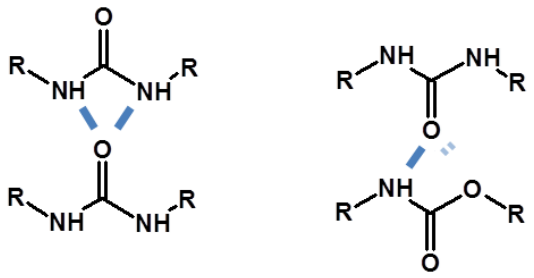

Figure 2.1. Comparison of hydrogen bonding in polyureas and polyurethanes.

In this study, segmental modification of polyurea chemistry was used to identify compositions that maintained target mechanical properties without gelation. Given the expense of peptides and the potentially confounding impact on phase morphology and mechanical properties, model polyurea compounds without peptide were investigated to elucidate key structure-property relationships prior to synthesis of peptide-based polyureas. The effect of increasing hard segment content on tensile strength was investigated in conjunction with the effect of chain extender chemistry on hydrogen bonding and gelation. Candidate hard segment content and chemistry selected from these studies was then used in a subsequent study focused on determining the effect of soft segment chemistry on polyurea morphology and mechanical properties. Overall, the methodology developed in these studies was used to identify candidate compositions with suitable mechanical properties for subsequent biodegradable formulation testing.

2.2 Materials

Polyether diamines (M_n=1700-2000 Da) were acquired from Huntsman Corporation®, **Figure 2.4.** Poly(ethylene glycol) (PEG) based polyether diamine, (trade name ED-2003, M_n=2000 Da), poly(propylene glycol) (PPG) polyether diamine, (trade name D-2000, M_n=2000 Da), poly(tetramethylene glycol) (PTMG) polyether diamine, (trade name XTJ-548, M_n=1700 Da) were used. Polymers were azeotropically dried by dissolving in toluene at a concentration of 100 mg/mL and then removed by rotary evaporation at 100 °C. Note that ED-2003 is predominantly comprised of PEG (n≈39), but is capped with ~3 repeat units of PPG adjacent to each amine end group. The XTJ-

548 also has a slightly lower M_n and contains a fraction of secondary amines according to the manufacturer. Hexane diisocyanate HDI, ethylene diamine (EDA), 1,2-diaminopropane (2DAP), 1,3-diaminopropane (3DAP), and lithium bromide (LiBr) were obtained from Sigma Aldrich and used as received. Anhydrous dimethylformamide (DMF) was obtained from Sigma Aldrich and stored over molecular sieves.

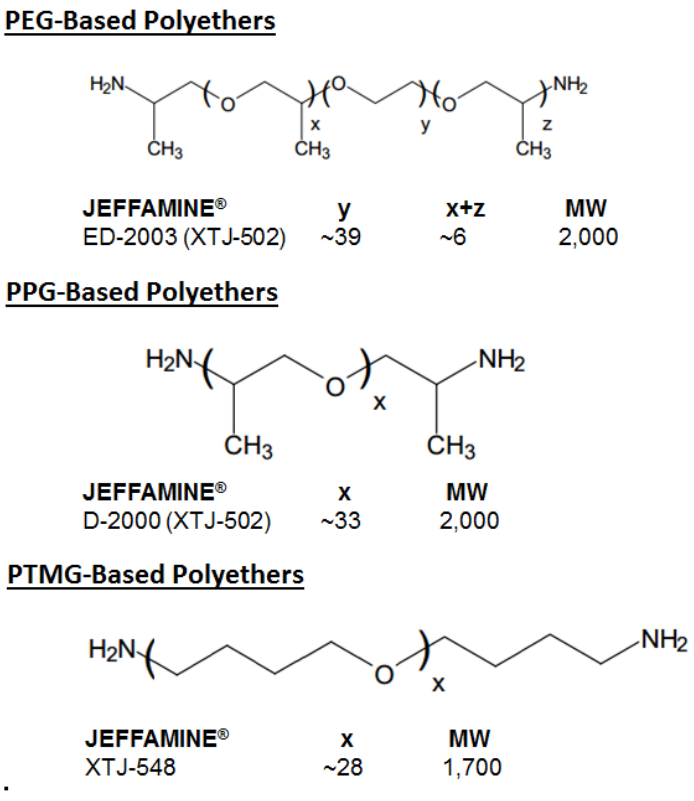

Figure 2.2. Candidate polymers used as the polyurea soft segment.

2.3 Methods

Polyureas were created in a one-pot synthesis with serial addition of reagents. Reactions were performed in a reaction vessel under a dry blanket of nitrogen gas with vigorous stirring. Polyether diamines were dissolved in DMF at a concentration of 25 mg/mL. The polymer solution was then added to a 50 mg/mL solution of HDI in DMF, forming the diisocyanate-functionalized prepolymer. A 10 mg/mL solution of the chain extender in DMF was then added drop-wise to build molecular weight, **Figure 2.3**.

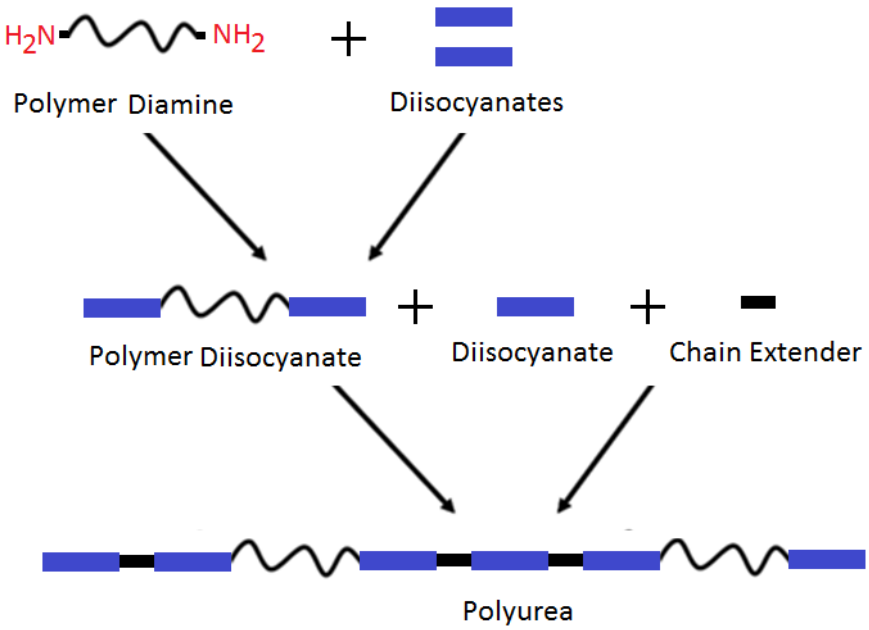

Figure 2.3. Synthesis of model biostable polyureas.

Fourier transform infrared (FTIR) spectroscopic analysis was performed on a Bruker TENSOR 27 spectrometer to confirm reaction completion and extent of hydrogen bonding. Polymer solutions were cast onto glass petri dishes at 50°C under a

nitrogen blanket and dried under vacuum starting at -200 mbar relative to atmosphere and then decreasing 200 mbar every 6 hours followed by full vacuum at 0 mbar for 24 hours. Resulting films were approximately 0.2 mm in thickness. Molecular weight was determined by gel permeation chromatography using a Viscotek GPCMax using Phenomenex columns with 10^3 Å, 10^4 Å, and 10^5 Å pores, with a mobile phase of DMF with 0.05 M LiBr. GPC samples were acquired by diluting 100 µL samples of the reaction solution in 900 µL of DMF with 0.1 M LiBr at 80ºC for 1 hour. Not all polymer solutions were sufficiently dissolved to perform GPC analysis. Dynamic mechanical analysis (DMA) was performed on film strips of approximately 5 mm × 22 mm × 0.2 mm in size using a TA Instruments RSA3 instrument. Temperature sweep tests were performed from -90°C to 150°C with a heating rate of 5°C/min with a 200 g load cell. Finally, dogbone specimens were cut from films for tensile testing with an Instron 3345 Single Column Universal Testing System equipped with a 1 kN load cell and 250 N pneumatic grips, tested at 100% strain/minute. Percent recovery was measured after specimens were strained to failure.

2.4 Results and Discussion

2.4.1 Effect of Increased Hard Segment Content on Mechanical Properties

Due to the high degree of hydrogen bonding found in polyureas, compositions approaching 15% HS content would commonly gel and become unprocessable and unusable. Therefore, HS content was first modulated from 10 to 14 wt% to determine the resulting effect on polyurea mechanical properties. A table of reagents is provided,

Table 2.1. Syntheses of polyureas with altered HS content were performed as previously described using PEG based soft segments due to their established use in tissue engineering constructs. Polyurea solutions varied in viscosity from a liquid to semi-solid. FTIR spectroscopy was used to confirm reaction completion and degree of hydrogen bonding, **Figure 2.4**. Spectra were baseline corrected and normalized to the ether backbone (1080 cm^{-1}) as an internal reference for hard segment content. Spectral analysis indicated full reaction completion as evidenced by loss of the isocyanate peak (2260 cm^{-1}). Significant urea formation was observed (1650 cm^{-1}), as well as hydrogen-bonded urea (1617 cm^{-1}), both intensify with increasing HS content. In samples with higher HS content, hydrogen bonded N-H groups were also observed (3500 cm^{-1}).

Table 2.1. Reactants in PEG based polyureas with 10%, 12%, and 14% HS content.

PU-10HS	Molecular Weight (kDa)	Grams	mL	molar ratio	mmols
PEG Diamine	2000	1.650	1.650	1.00	0.825
HDI (total)	168.2	0.172	0.164	1.24	1.023
EDA	60.1	0.012	0.013	0.24	0.198

PU-12HS	Molecular Weight (kDa)	Grams	mL	molar ratio	mmols
PEG Diamine	2000	1.650	1.650	1.00	0.825
HDI (total)	168.2	0.203	0.194	1.46	1.2045
EDA	60.1	0.023	0.026	0.46	0.3795

PU-14HS	Molecular Weight (kDa)	Grams	mL	molar ratio	mmols
PEG Diamine	2000	1.650	1.650	1.00	0.825
HDI (total)	168.2	0.235	0.224	1.69	1.3943
EDA	60.1	0.034	0.039	0.69	0.5693

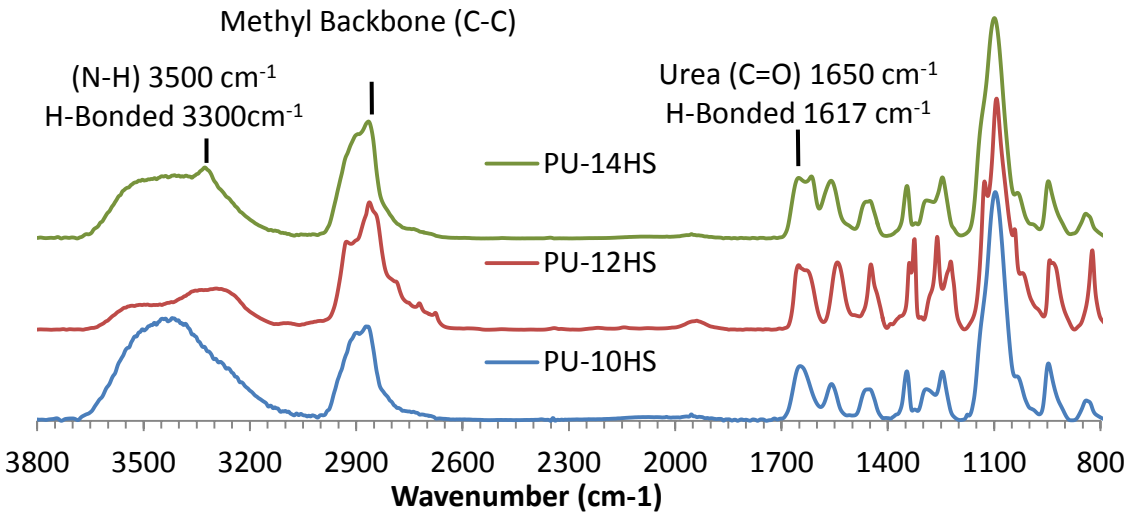

Figure 2.4. FTIR spectra of PEG polyureas containing 10%, 12%, and 14% HS content.

The stress–strain behavior of polyureas with increased HS content is similar to a semi-crystalline polymer above its Tg.[204] Polyureas displayed a yield point followed by drawing similar to semi-crystalline PEG polyurethanes reported in the literature.[132,205-207] Polyureas with 10% HS were characterized by a 2% secant modulus of 30.1 MPa ± 6.7 MPa, an ultimate elongation before failure of 1150% ± 10%, and an ultimate tensile strength of 10.6 MPa ± 1.5 MPa. Polyureas with 12% HS were characterized by a 2% secant modulus of 43.8 MPa ± 6.6 MPa, an ultimate elongation before failure of 1150% ± 60%, and an ultimate tensile strength of 13.8 MPa ± 0.6 MPa. Polyureas with 14% HS were characterized by a 2% secant modulus of 49.2 MPa ± 4.1 MPa, an ultimate elongation before failure of 1230% ± 10%, and an ultimate tensile strength of 24.2 MPa ± 0.5 MPa, **Figure 2.5, Table 2.2.** The increase in modulus and tensile strength was attributed to the increase in HS content. Previous literature has shown that increased HS

content puts greater constraint on the soft segment matrix, leading to a higher initial modulus.[126,134] Several studies have attributed enhanced tensile properties to both increased phase separation and soft segment crystallinity.[207,208] All polyureas were observed to have a significant permanent set with percent recovery calculated to be 298% ± 28% for polyureas with 10% HS, 352% ± 23% for polyureas with 12% HS, and 398% ± 36% for polyureas with 14% HS. Given the relative high recovery of other polyether-based polyurethanes, the permanent set was attributed to the deformation of soft segment crystalline domains.

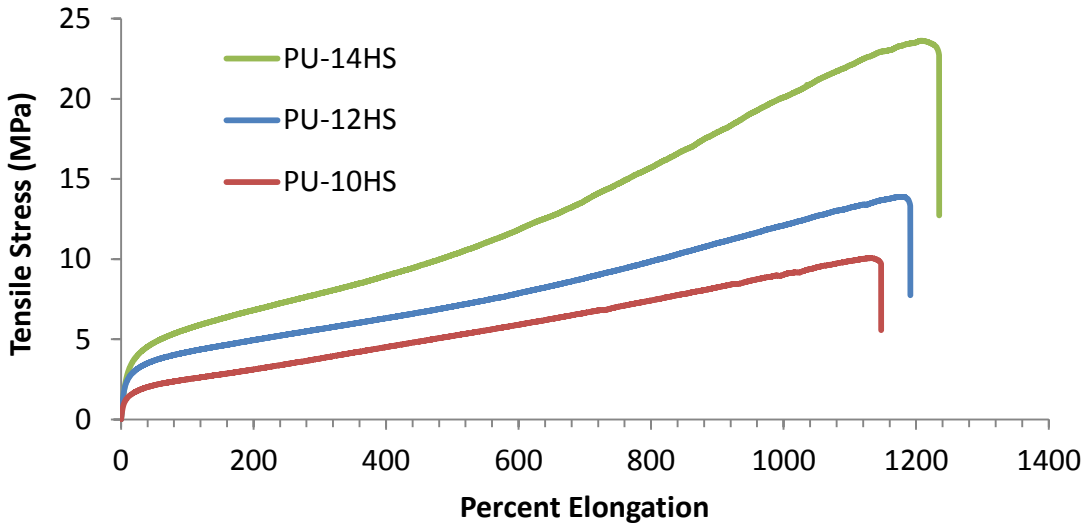

Figure 2.5. Stress-strain response of PEG polyureas with 10%, 12%, and 14% HS content.

Table 2.2. Tensile properties of polyureas with 10%, 12%, and 14% HS content.

Polyurea	Modulus (MPa)	Elongation (%)	Strength (MPa)	Permanent Set (%)
PU-10HS	30.1 ± 6.7	1150 ± 10	10.6 ± 1.5	298 ± 28
PU-12HS	43.8 ± 6.6	1150 ± 60	13.8 ± 0.6	352 ± 23
PU-14HS	49.2 ± 4.1	1230 ± 10	24.2 ± 0.5	398 ± 36

2.4.2 Effect of Registry on Hydrogen Bonding and Gelation

Preliminary studies indicated that HS content of 15% was the threshold for gelation in PEG based polyureas. PPG based polyureas were even more difficult to synthesize and were unable to reach 10% HS content without gelation. Given that improved tensile properties were observed at higher hard segment contents, additional studies were conducted in an effort to prevent gelation at higher hard segment contents and extend pot life. To this end, PEG based polyurea compositions were formulated to explore the effect of HS registry on hydrogen bonding and the corollary effects on gelation. Based on preliminary studies, 15% HS content was selected for these studies. Chain extender composition was modulated to investigate the effect of HS registry with mixed symmetry (A), mixed length (B), and/or sterically-hindered diamines (C), **Figure 2.6.**

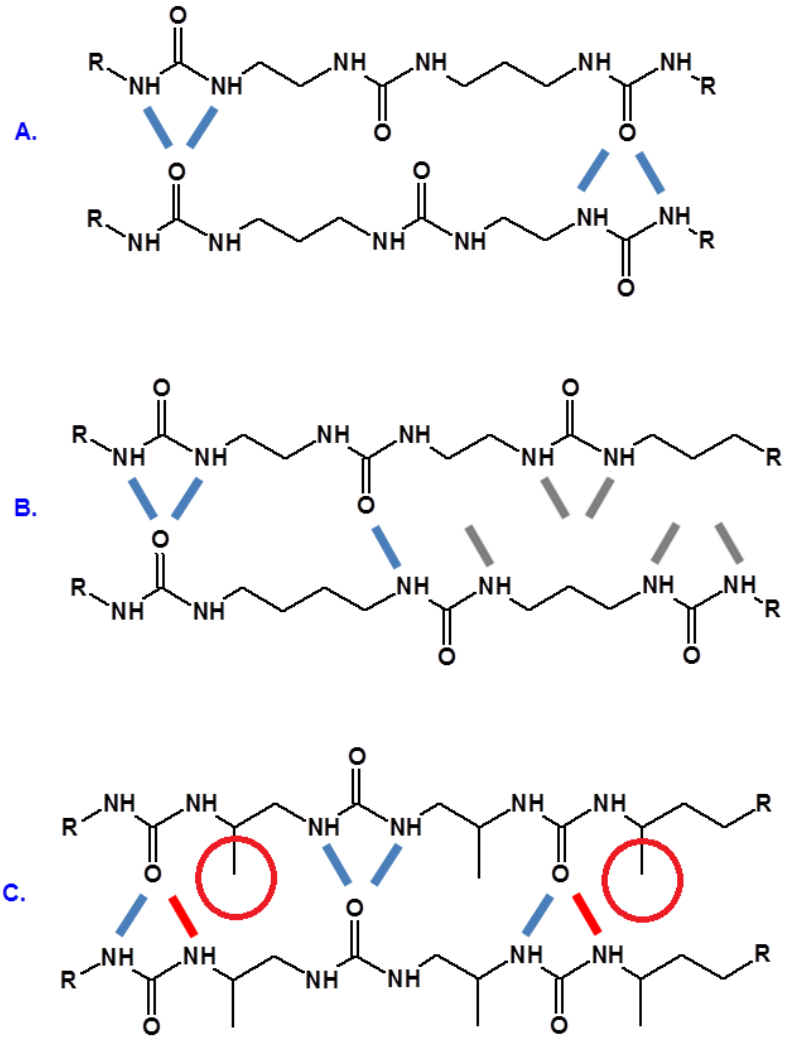

Figure 2.6. HS registry resulting from altered chain extender chemistry using: mixed symmetry (A), mixed length (B), and/or sterically-hindered diamines (C).

Syntheses of polyureas were performed as previously described using PEG based soft segments with altered HS chemistry. Resulting polyurea solutions varied in viscosity from a viscous liquid to a semi-solid. Polyureas were formulated to test mixed length (EDA and BDA), mixed symmetry (EDA and 3DAP), and a combination of mixed length, symmetry, and sterically-hindering groups (2DAP and 3DAP) compared

to polyureas utilizing EDA alone. A table of reagents is provided, **Table 2.3**. All polyureas with the exception of those made with a combination of 2DAP and 3DAP increased in viscosity (gelled) such that cast films resulted in cracked, unusable films. FTIR spectral analysis was performed as described previously to determine the effect of chain extender chemistry on the degree of hydrogen bonding. All spectra displayed significant hydrogen bonding of the urea hard segment (1617 cm^{-1}), **Figure 2.7.** It was found that polyureas chain extended entirely with EDA had the highest viscosity and almost all urea displayed hydrogen bonding (1617 cm^{-1}). Polyureas created with a 1:1 mixture of the even-length diamines EDA and BDA had the next highest viscosity as well as a shoulder at 1617 cm^{-1}, indicating a measure of hydrogen bonding. Polyureas created with a 1:1 mixture of EDA and 3DAP, varying length and symmetry, showed similar viscosity to the EDA-BDA mixture and a small increase in hydrogen bonding. Polyureas synthesized using a 1:1 mixture of 2DAP and 3DAP had the lowest viscosity and minimal evidence of hydrogen bonding. Polyureas using this mixture of 2DAP and 3DAP were the only solutions found to make cohesive films via film casting. It was hypothesized that this mixture of diamines with different length, symmetry, and sterically-hindering groups had an additive effect, reducing hydrogen bonding better than the other formulations alone. This formulation was able to prevent gelation and improve processability.

Table 2.3. Reactants in PEG based polyureas containing chain extender mixtures of EDA, BDA, 2DAP, and 3DAP.

PU-EDA	Molecular Weight (kDa)	Grams	mL	molar ratio	mmols
PEG Diamine	2000	3.305	3.305	1.0000	1.6523
HDI (total)	168.2	0.549	0.525	1.6800	3.2656
EDA	60.1	0.040	0.045	0.3400	0.6609

PU-EDA-BDA	Molecular Weight (kDa)	Grams	mL	molar ratio	mmols
PPG Diamine	2000	3.305	3.305	1.0000	1.6523
HDI (total)	168.2	0.507	0.484	1.5500	3.0129
EDA	60.1	0.032	0.036	0.2750	0.5346
BDA	88.15	0.047	0.054	0.2750	0.5346

PU-EDA-3DAP	Molecular Weight (kDa)	Grams	mL	molar ratio	mmols
PTMG Diamine	1700	3.305	3.305	1.0000	1.9438
HDI (total)	168.2	0.513	0.490	1.5700	3.0518
3DAP	74.12	0.041	0.046	0.2850	0.554
EDA	60.1	0.033	0.038	0.2850	0.554

PU-2DAP-3DAP	Molecular Weight (kDa)	Grams	mL	molar ratio	mmols
PTMG Diamine	1700	3.305	3.305	1.0000	1.9438
HDI (total)	168.2	0.507	0.484	1.5500	3.0129
3DAP	74.12	0.040	0.045	0.2750	0.5346
2DAP	74.13	0.040	0.046	0.2750	0.5346

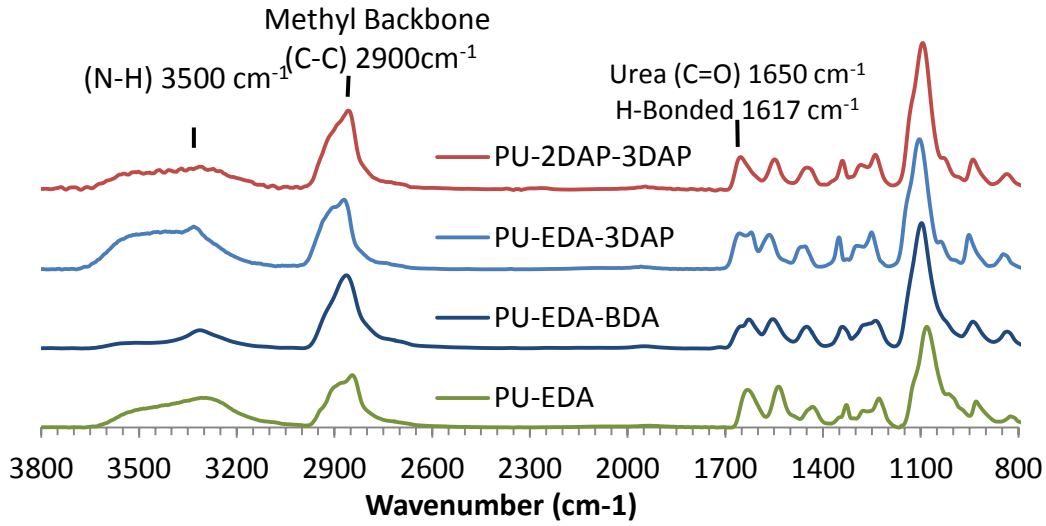

Figure 2.7. FTIR spectra of PEG based polyureas containing chain extender mixtures of EDA, BDA, 2DAP, and 3DAP

2.4.3 Effect of Soft Segment Chemistry on Morphology and Mechanical Properties

The mixture of 2DAP and 3DAP at 15% HS content was selected for subsequent testing of the effect of soft segment chemistry due to its ability to reduce hydrogen bonding and prevent gelation. Polyureas with alternate soft segment chemistries were synthesized as described previously using PEG, PPG, and PTMG diamine based soft segments to investigate the effect on polyurea structure on morphology and mechanical properties. A Table of reagents is provided, **Table 2.4**. There was no evident difference in polyurea solution viscosity. FTIR spectral analysis was used as described above to assess hydrogen bonding, **Figure 2.8**. PEG polyureas were found have the least hydrogen bonding, followed by PPG, and PTMG. In addition to hydrogen bonding of the urea carbonyl, hydrogen bonding of N-H groups was observed (3500 cm^{-1}) and more

pronounced in PPG and most in PTMG based polyureas. The presence of hydrogen bonded N-H stretching with decreased hydrogen bonded urea indicates that a portion of the hydrogen bonding can be attributed to interactions between the hard segment and soft segment.[209,210] The reduced number of ether linkages in PTMG relative to PEG and PPG is thought to reduce the number of hydrogen bond acceptors and therefore reduce the propensity for hard segments to hydrogen bond with soft segments. FTIR indicates PPG has slightly higher HB urea, which is attributed its hydrophobicity, which has been shown to increase phase separation HB urea.[210]

Table 2.4. Reactants in PEG, PPG, and PTMG polyureas containing 15% HS content.

PU-PEG	Molecular Weight (kDa)	Grams	mL	molar ratio	mmols
PEG Diamine	2000	3.305	3.305	1.0000	1.6523
HDI (total)	168.2	0.579	0.553	1.7700	3.4406
3DAP	74.12	0.055	0.062	0.3850	0.7484
2DAP	74.13	0.055	0.064	0.3850	0.7484

PU-PPG	Molecular Weight (kDa)	Grams	mL	molar ratio	mmols
PPG Diamine	2000	3.305	3.305	1.0000	1.6523
HDI (total)	168.2	0.579	0.553	1.7700	3.4406
3DAP	74.12	0.055	0.062	0.3850	0.7484
2DAP	74.13	0.055	0.064	0.3850	0.7484

PU-PTMG	Molecular Weight (kDa)	Grams	mL	molar ratio	mmols
PTMG Diamine	1700	3.305	3.305	1.0000	1.9438
HDI (total)	168.2	0.507	0.484	1.5500	3.0129
3DAP	74.12	0.040	0.045	0.2750	0.5346
2DAP	74.13	0.040	0.046	0.2750	0.5346

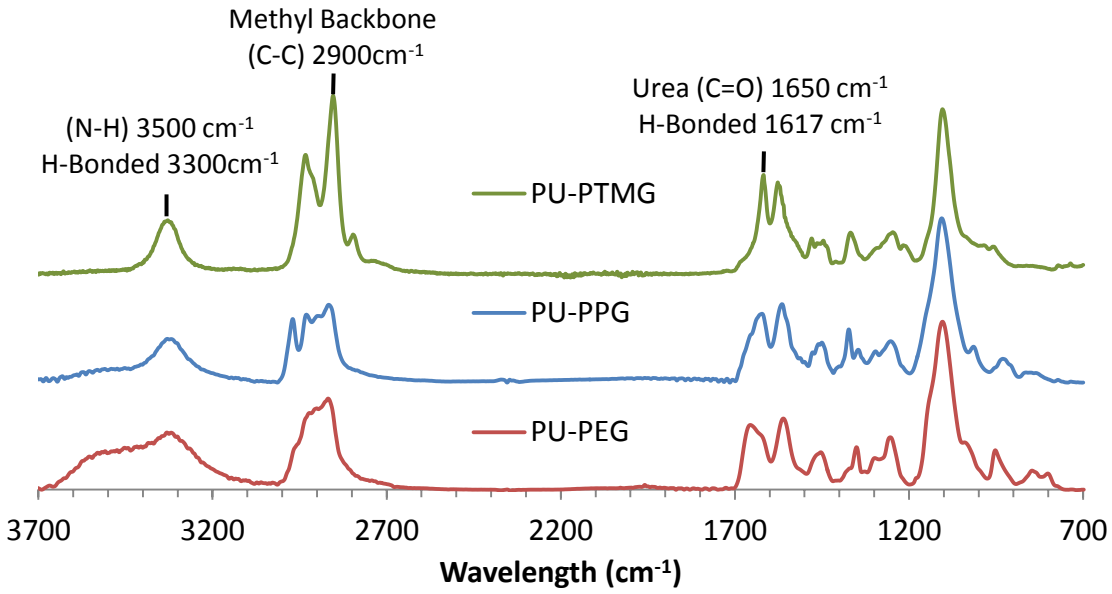

Figure 2.8. FTIR spectra of PEG, PPG, and PTMG polyureas with 15% HS content.

Dynamic mechanical analysis was performed to assess degree of phase separation of candidate polyureas, **Figure 2.9**. It was observed that PEG based polyureas had a broad Tg ranging from -40 ºC to 10 ºC, followed by a Tm at 37 ºC. PTMG and PPG based polyureas were found to have a sharp Tg at -55 ºC and -45 ºC, respectively. PTMG exhibited a Tm at 85 ºC, whereas PPG had no visible Tm within this range. The broad Tg of PEG based polyureas indicated possible phase mixing which correlates with the hydrogen bonding between the hard and soft segment seen in FTIR. The presence of a Tm at 37 °C in PEG polyureas indicates decreased mobility of the soft segment at room temperature, explaining plastic deformation as well as the need to cast films at elevated temperatures. PTMG based polyureas showed increased phase separation when compared to PEG polyureas, which is attributed to the reduction in hydrogen bonding

between the hard and soft segment and increased thermodynamic incompatibility between the more hydrophobic polymer and the polar hard segments.[210-212]

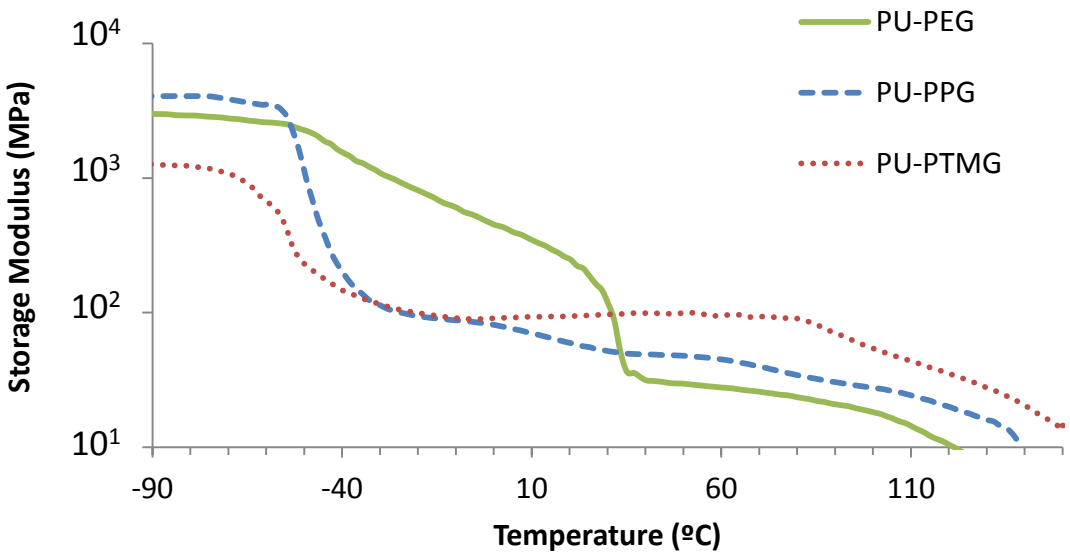

Figure 2.9. Dynamic mechanical analysis of PEG, PPG, and PTMG polyureas containing 15% HS content.

Stress strain plots were analyzed to investigate the impact of soft segment chemistry and the observed differences in morphology on tensile properties, **Figure 2.10**. PEG, PPG, and PTMG polyureas all displayed yield point, followed by drawing in PTMG and PEG based polyureas as discussed previously. PEG polyureas were characterized by a 2% secant modulus of 52.2 MPa ± 4.3 MPa, an ultimate elongation before failure of 1130% ± 20%, and an ultimate tensile strength of 25.4 MPa ± 4.9 MPa. PPG polyureas were characterized by a 2% secant modulus of 36.3 MPa ± 8.1 MPa, an

ultimate elongation before failure of 100% ± 10%, and an ultimate tensile strength of 5.4 MPa ± 1.1 MPa. PTMG polyureas were characterized by a 2% secant modulus of 87.6 MPa ± 9.1 MPa, an ultimate elongation before failure of 650% ± 60%, and an ultimate tensile strength of 17.1 MPa ± 6.7 MPa, **Figure 2.10.** Mechanical properties as well as molecular weight values are provided, **Table 2.5.** The high modulus and strength seen in PEG polyureas is attributed to its semicrystallinity discussed previously. PPG polyureas perform similarly, but break early around 100%. PPG's poor tensile strength is attributed to its low molecular weight relative to PTMG and PEG based polyureas, **Figure 2.11**. This has been attributed to its hydrophobicity causing premature phase separation and poor compositional homogeneity.[210] Low tensile strength for comparatively similar PPG based polyuretheanes is also well documented to be a result of the soft segment's inability to crystallize under strain.[210,213] While PEG based polyureas exhibit superior mechanical strength, they have poor recovery after failure, indicating the crystalline domains have undergone plastic deformation.

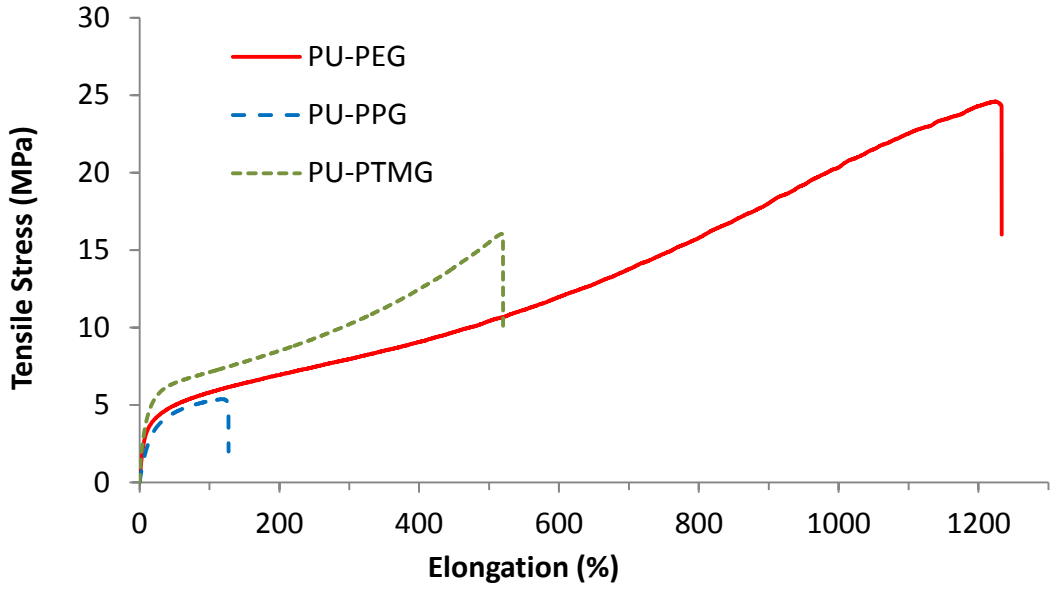

Figure 2.10. Stress-strain plots of PEG, PPG, and PTMG polyureas containing 15% HS content.

Table 2.5. Mechanical properties of PEG, PPG, and PTMG polyureas containing 15% HS content.

Polyurea	Modulus (MPa)	Strength (MPa)	Elongation (%)	Permanent Set (%)	M_w (kDa)	Polydispersity (M_w/M_n)
PU-PEG	52.2 ± 4.3	25.4 ± 4.9	1130 ± 20	352 ± 23	210 ± 13	2.61 ± 0.10
PU-PPG	36.3 ± 8.1	5.4 ± 1.1	100 ± 3	10 ± 3	72 ± 7	2.40 ± 0.21
PU-PTMG	87.6 ± 9.1	17.1 ± 6.7	650 ± 60	112 ± 8	231 ± 15	2.35 ± 0.14

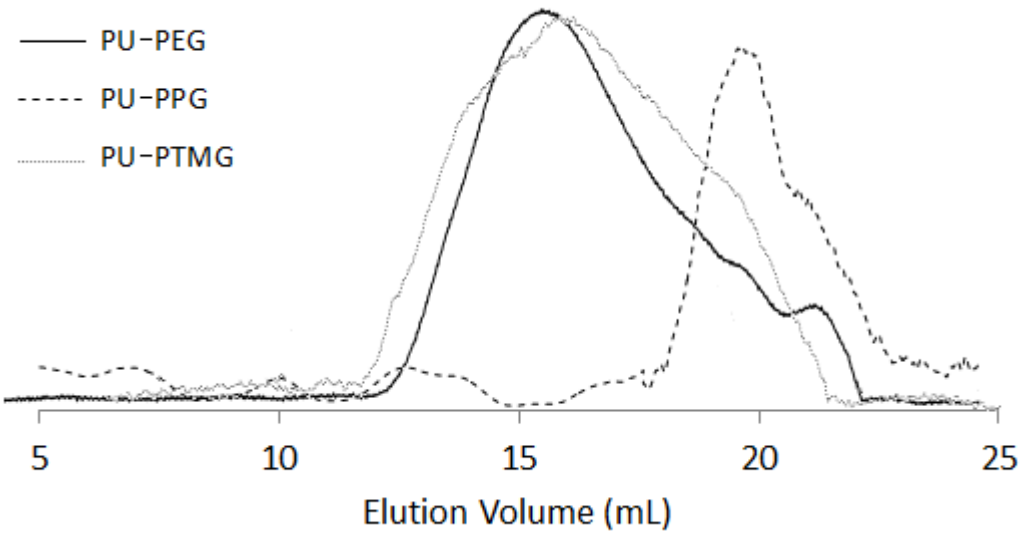

Figure 2.11 Molecular weight analysis of GPC PEG, PPG, and PTMG polyureas

2.5 Conclusions

PEG based polyurea formulations using EDA as the chain extender with HS content ranging from 10-14% were successfully synthesized and characterized. It was found that HS content displayed a positive correlation with modulus, elongation, and

tensile strength. Formulations with 14% HS was the maximum level achieved without gelation. Chain extender combinations of EDA and BDA, EDA and 3DAP, and 3DAP and 2DAP, were used to alter hard segment registry and modulate hydrogen bonding such that 15% HS polyureas could be synthesized without gelation. Polyurea formulations with different soft segment chemistries, PEG, PPG and PTMG, were synthesized and characterized to analyze the effect on morphology and mechanical properties. It was found that PPG based polyureas had very poor mechanical modulus, strength, and elongation and were thus inadequate as a candidate scaffold. PEG based polyureas had the highest tensile strength and elongation but poor elasticity. Notably, PEG-based polyureas swelled significantly in water with a dramatic loss of mechanical properties. PTMG based polyureas had tensile strengths beyond the target 10 MPa requirement as a ligament scaffold and did not absorb water in any significant amount. This formulation was selected for subsequent biodegradable polyurea testing.

CHAPTER III

BIODEGRADABLE POLYUREAS

3.1 Introduction

The majority of biodegradable, synthetic polymers used in tissue engineering scaffolds incorporate ester or anhydride linkages that degrade via hydrolysis. Success of ligament grafts depends upon (1) the construct retaining sufficient mechanical properties to stabilize the joint throughout remodeling; (2) the new tissue receiving the appropriate level of load for directed collagenous organization/alignment. It continues to be difficult to both predict and tailor the non-specific hydrolysis of current synthetic biomaterials; whereas, natural materials are limited by mass-production, variability, or lack the tensile properties necessary for ligament applications. Therefore, new biomaterials are needed that can meet the complex design criteria necessary for ligament repair.

Collagen-mimetic polyureas have the potential to combine the strength and tunability of synthetic elastomers with the cell-responsive degradation of native collagen. System-responsive degradation of a collagen-mimetic peptide isolated to the soft segment would integrate polyurea biodegradation with native ligament remodeling. By yielding control of scaffold degradation to the cell, the scaffold will degrade at a rate that best promotes tissue formation and organization. To this end, the MMP-2 sensitive peptide, GPQGIWGQGK, was identified as an efficient route for cell-responsive scaffold degradation[214]. Proteolytically degradable peptides such as this have been used in tissue engineering scaffold such as hydrogels, but have not yet been utilized in load bearing scaffold such as elastomers[215]. We hypothesize that incorporation of this

collagen oligopeptide into the soft segment of the polyurea elastomer will decouple the degradation rate and mechanical properties of these new biomimetic polymers.

For this portion of the study, a polyurea elastomer was synthesized that incorporates the selected collagen-derived peptide into the backbone of the polymer chain, **Figure 3.1.** A triblock soft segment structure was designed with PTMG on the two ends and a short PEG linker unit in the center that to serve as an analog for the peptide. For biodegradable formulations, a percentage of this PEG linker is substituted for the peptide which is approximately equivalent in molecular weight and similar in hydrophilicity. This is expected to result in minimal changes to the phase separated morphology and corollary mechanical properties of the polyurea. To test this hypothesis, polyureas with varying levels of peptide were characterized to determine the effect of the peptide on morphology, mechanical properties, and rate of enzymatic degradation.

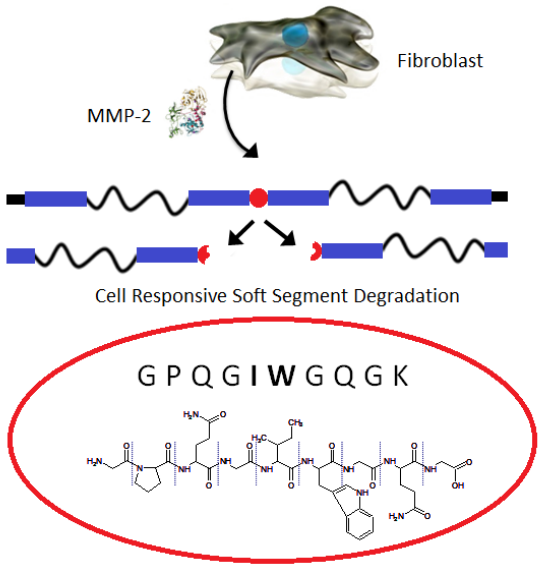

Figure 3.1. Cell responsive degradation mechanism in biodegradable polyureas

3.2 Materials

Polyether diamines were acquired from Huntsman Corporation. PEG based polyether diamine, (RE-900, M_n=900 Da), and PTMG diamine, (XTJ-548, M_n=1700) were used. Polymers were azeotropically dried by dissolving in Toluene at a concentration of 100 mg/mL, and then removed by rotary evaporation at 100°C. Hexane diisocyanate HDI, ethylene diamine (EDA), 1,2-diaminopropane (2DAP), 1,3-diaminopropane (3DAP), and lithium bromide (LiBr) were obtained from Sigma Aldrich and used as received. Anhydrous dimethylformamide (DMF) was obtained from Sigma Aldrich, and stored over molecular sieves. PBS and Pen-Strep solution (10,000 meq/mL, 10 mg/mL) were obtained from Sigma Aldrich and used as received. Collagenase type 4 was obtained from Worthington Biochemical Corporation Lakewood, NJ and used as received.

3.3 Methods

Biodegradable polyureas were synthesized in a manner similar to the biostable formulations. Polyureas had 15% HS content, composed of a 1:1 mixture of 2DAP and 3DAP, in order to maximize mechanical properties while reducing the potential for gelation. PTMG based soft segments were selected because of their mechanical strength, hydrophobicity, and elasticity. The reaction scheme was modified in order to incorporate

the PEG oligomer. For biodegradable formulations, 10% or 20% of this PEG oligomer was substituted for the peptide. HS content was calculated from the HDI and diamines located in the HS blocks; this did not include HDI linking soft segment blocks. A table of reagents is provided, **Table 3.1.**

Fourier transform infrared (FTIR) spectroscopic analysis was performed on a Bruker TENSOR 27 spectrometer to confirm reaction completion, extent of hydrogen bonding, and incorporation of the peptide. Reacted polymer solutions were cast onto glass petri dishes at 50 °C under partial, increasing vacuum (under a nitrogen blanket, starting at -200 mbar relative to atmosphere, decreasing 200 mbar every 6 hours, followed by full vacuum at 0 mbar for 24 hours) to a thickness of approximately 0.2 mm for tensile testing with an Instron 3345 Single Column Universal Testing System equipped with a 1 kN load cell and 250 N pneumatic grips, tested at 100% strain/minute. Dynamic mechanical analysis (DMA) was performed using a TA Instruments RSA3 instrument to investigate relative phase separation. Temperature sweep tests were performed from -90°C to 150°C with a heating rate of 5°C/min with a 200 g load cell.

Polymer films were subjected to enzymatic degradation for up to 4 weeks and then examined for chemical, mechanical, and visual changes, (n=3). Specimens were submerged in 37 °C PBS solution with or without collagenase (10 mg/mL). All solutions contained 1% Pen-Strep solution to prevent microbial contamination. Solutions were changed and specimens were weighed weekly. Uniaxial tensile testing of samples took place 2 weeks and 4 weeks and were compared to control specimens. Scanning electron microscopy (SEM) was used to inspect polyurea films for surface damage.

Table 3.1. Reactants in PTMG based polyureas containing 15% HS content and 0%, 10%, and 20% peptide content.

PU-0PEP	Molecular Weight (kDa)	Grams	mL	molar ratio	mmols
PTMG Diamine	1700	3.500	3.500	1.0000	2.0588
HDI (total)	168.2	0.984	0.940	2.8410	5.8491
PEG(900)NH2	900	0.926	0.926	0.500	1.0294
Peptide	1026	0.000	0.000	0.000	0
3DAP	74.12	0.102		0.6705	1.3804
2DAP	74.13	0.102	0.118	0.6705	1.3804

PU-10PEP	Molecular Weight (kDa)	Grams	mL	molar ratio	mmols
PTMG Diamine	1700	3.500	3.500	1.0000	2.0588
HDI (total)	168.2	0.984	0.940	2.8410	5.8491
PEG(900)NH2	900	0.834	0.834	0.450	0.9265
Peptide	1026	0.106	0.106	0.050	0.1029
3DAP	74.12	0.102	0.115	0.6705	1.3804
2DAP	74.13	0.102	0.118	0.6705	1.3804

PU-20PEP	Molecular Weight (kDa)	Grams	mL	molar ratio	mmols
PTMG Diamine	1700	3.500	3.500	1.0000	2.0588
HDI (total)	168.2	0.984	0.940	2.8410	5.8491
PEG(900)NH2	900	0.741	7.412	0.400	0.8235
Peptide	1026	0.211	0.211	0.100	0.2059
3DAP	74.12	0.102	0.115	0.6705	1.3804
2DAP	74.13	0.102	0.118	0.6705	1.3804

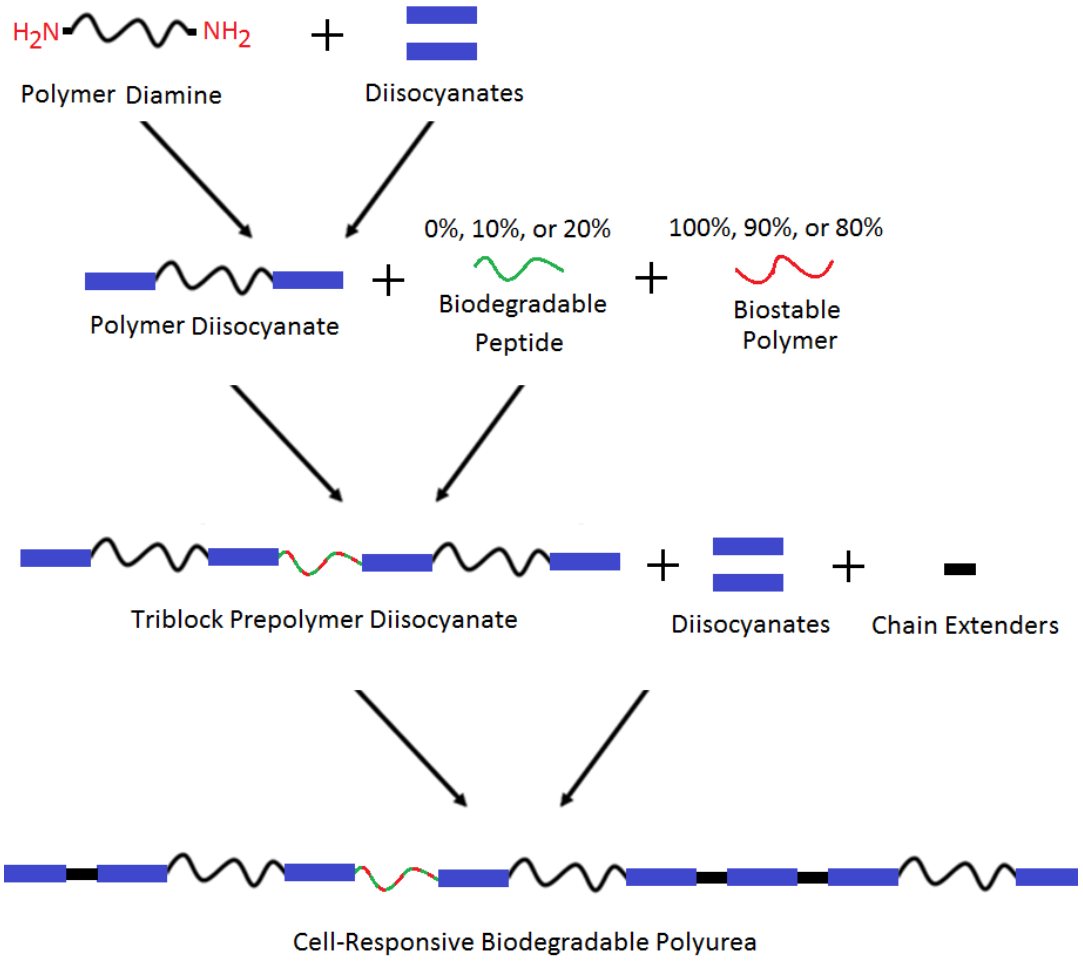

Figure 3.2. Synthetic design of cell-responsive, biodegradable polyureas.

3.4 Results and Discussion

3.4.1 Effect of Peptide on Morphology and Mechanical Properties

FTIR spectra of polymer films contained peaks correlating to hydrogen bonded N-H stretching (3300 cm^{-1}), the methyl backbone of PTMG and PEG (2900 cm^{-1}), amide from the peptide, (C=O, 1660 cm^{-1}, various intensities), urea (1650 cm^{-1}), hydrogen bonded urea (1617 cm^{-1}), and the ether backbone of PTMG and PEG (1080 cm^{-1}), **Figure 3.3.** Although the peptide peak is convoluted by the urea peak, a trend was observed that indicated successful peptide incorporation. A shoulder at 1660 cm^{-1} assigned to the amide of the peptide can be seen to increase with increaing peptide content. Additionally, subtracting the 0% peptide as a baseline, intensities at 1660 cm^{-1} are observed to be at relative ratios of 1:1.76 for 10% and 20% peptide content, respectively. The presence of HB urea suggests that the peptide did not disrupt the two phase morphology.

DMA plots of polyureas with varying peptide content are compared in **Figure 3.4**. A broadening of the glass transition (Tg) with increasing peptide content was observed and was attributed to an increase in phase mixing. Given that the peptide contains many amide groups which function as hydrogen bond donors (N-H) and acceptors (C=O), it was hypothesized that the peptide provided an increased opportunity for hydrogen bonding between the hard and soft segments.

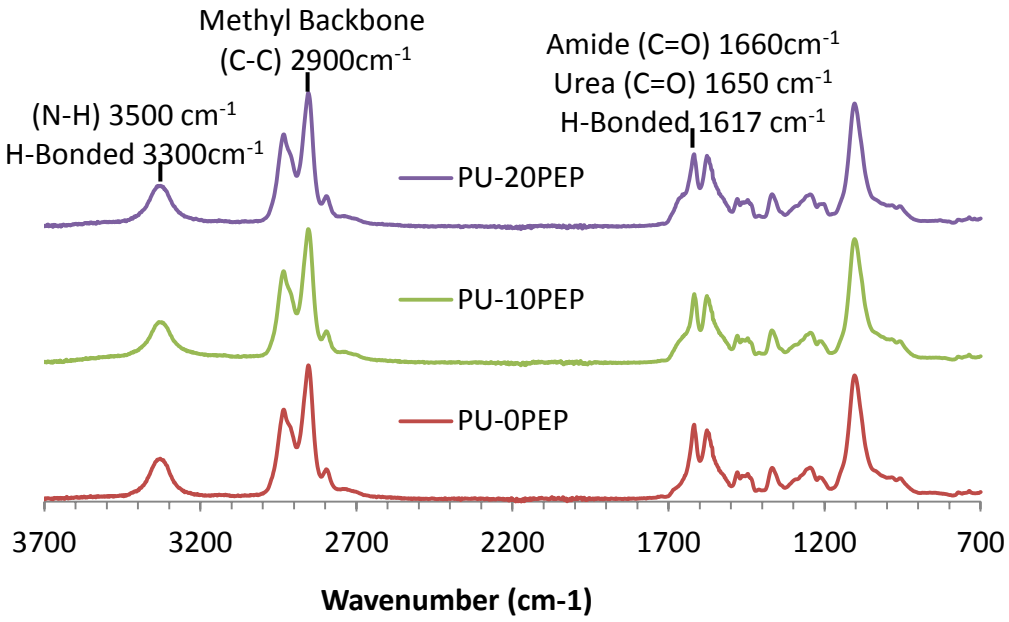

Figure 3.3 FTIR spectra of PTMG based polyureas containing 15% HS content and 0%, 10%, or 20% peptide content.

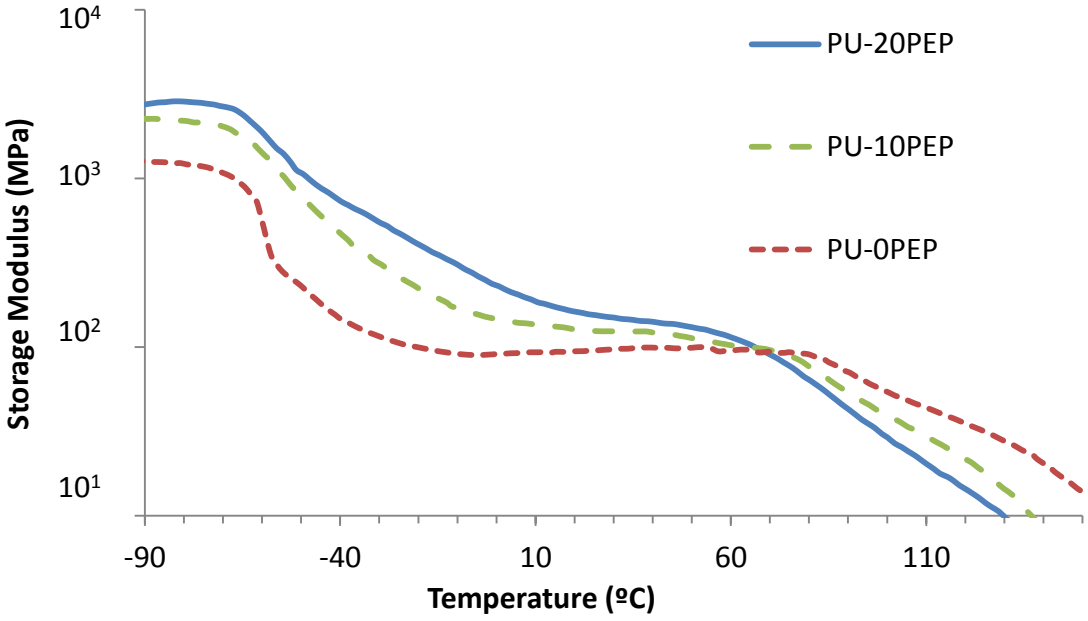

Figure 3.4 Dynamic mechanical analysis of PTMG polyureas with 15% HS content and 0%, 10%, or 20% peptide content.

Stress strain plots were analyzed to investigate the impact of the peptide and its observed differences in morphology on tensile properties, **Figure 3.5**. PTMG polyureas all displayed a yield point, followed by drawing as discussed previously. Polyureas with 0% peptide were characterized by a 2% secant modulus of 25.3 MPa ± 0.8 MPa, an ultimate elongation before failure 310% ± 20%, and an ultimate tensile strength of 7.2 MPa ± 0.2 MPa. Polyureas with 10% peptide were characterized by a 2% secant modulus of 43.0 MPa ± 2.9 MPa, an ultimate elongation before failure of 390% ± 10%, and an ultimate tensile strength of 7.6 MPa ± 0.4 MPa. Polyureas with 20% peptide were characterized by a 2% secant modulus of 45.4 MPa ± 1.3 MPa, an ultimate elongation before failure of 510% ± 10%, and an ultimate tensile strength of 10.8 MPa ± 0.3 MPa, **Figure 3.5.** A table of mechanical properties is provided, **Table 3.2.** Overall, tensile properties of polyureas with varying peptide content showed increased tensile strength and elongation with increasing peptide content, **Figure 3.5.** The increase in phase mixing evident in the DMA with increasing peptide content was hypothesized to have been a result of the peptide hydrogen bonding with the hard segment. This increased phase mixing permitted continued chain organization and strain induced crystallization, resulting in increased ultimate tensile strength.

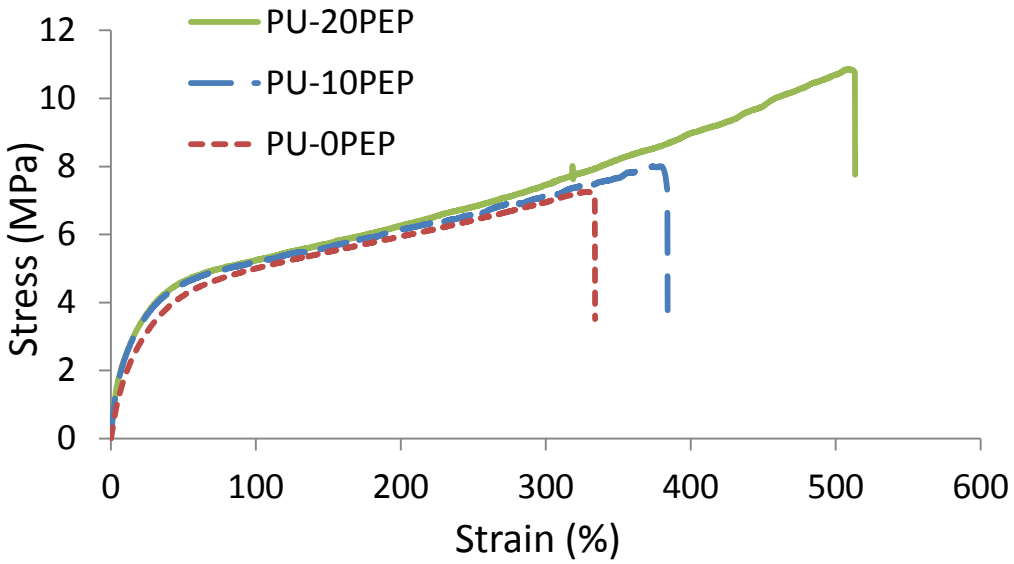

Figure 3.5 Stress-strain behavior of PTMG based polyureas containing 15% HS content and 0%, 10%, or 20% peptide content.

Table 3.2. Tensile properties of untreated polyureas.

	Modulus (MPa)	Elongation (%)	Strength (MPa)
PU-0PEP	25.3 ± 0.8	310 ± 20	7.2 ± 0.2
PU-10PEP	43 ± 2.9	390 ± 10	7.6 ± 0.4
PU-20PEP	45.4 ± 1.3	510 ± 10	10.8 ± 0.3

3.4.2 Enzymatic Degradation of Biodegradable Polyureas

Polymer films were subjected to degradation in collagenase solutions over 4 weeks. Fourier transform infrared (FTIR) spectroscopic analysis was used to evaluate peptide degradation, **Figure 3.6**. A detailed view of the carbonyl region of the polyureas is also provided, **Figure 3.7.** No evidence of degradation was observed for control

specimens, as expected. A decrease in peak height at 1660 cm^{-1} assigned to the peptide was observed after 4 weeks of degradation in polyureas with 20% peptide content; however, no corollary decrease was discernible in polyureas with 10% peptide content. Subtracting the 0% peptide as a baseline, polyureas with 20% peptide content experienced a 40% reduction in the peak at 1660 cm^{-1} indicating possible chain scission of the peptide and extraction of low molecular weight species. No spectral changes were detected in polyureas with 10% or 20% peptide when subject to degradation in PBS without collagenase. This indicates that the changes were specific to enzymatic chain scission.

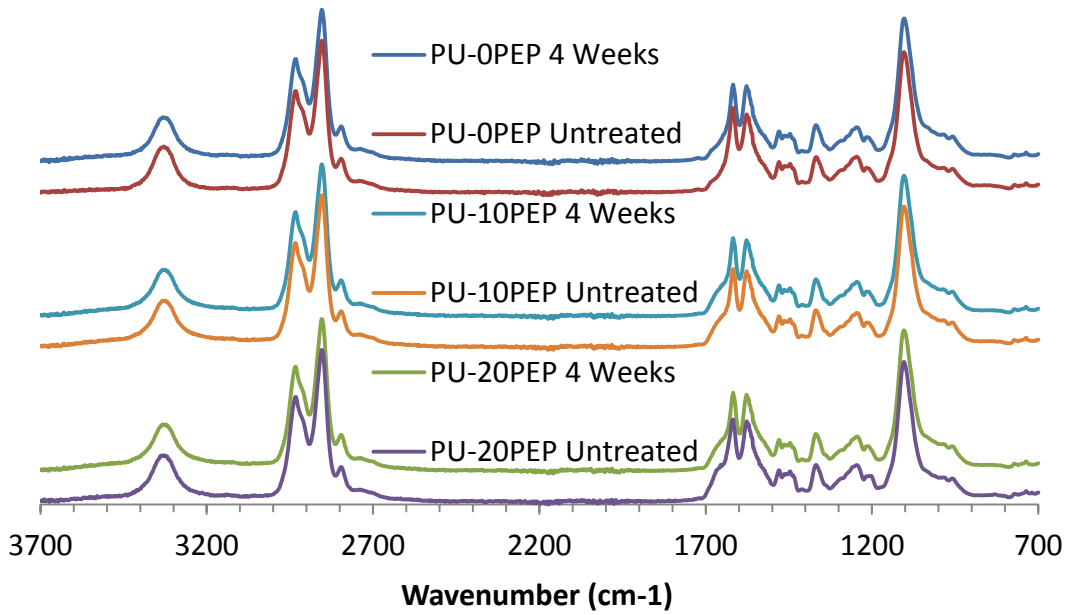

Figure 3.6 FTIR analysis of PTMG based polyureas containing 15% HS content and 0%, 10%, and 20% peptide content after 4 weeks of degradation in PBS/collagenase.

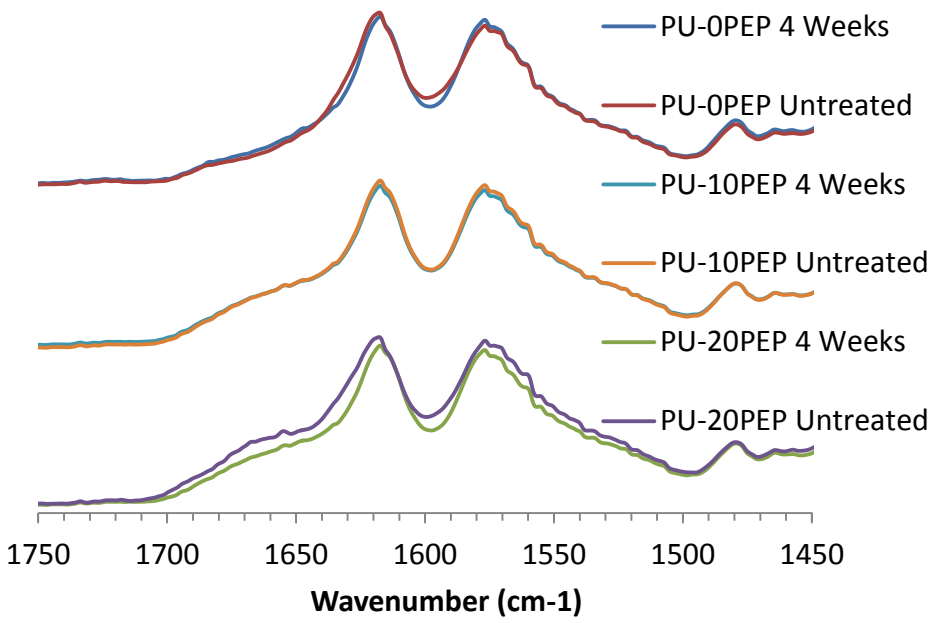

Figure 3.7 FTIR analysis of PTMG based polyureas containing 15% HS content and 0%, 10%, and 20% peptide content after 4 weeks of degradation in PBS/collagenase (carbonyl region).

Stress strain plots of specimens subjected to 4 weeks of degradation were analyzed to investigate the impact of degradation on tensile properties, **Figure 3.8, 3.9, 3.10**. Polyureas displayed a yield point, followed by drawing and in some instances a degree of strain induced crystallization. A complete table of values obtained from the degradation study is included, **Table 3.3.** This table features modulus, elongation, and strength for polyureas with 0%, 10%, and 20% peptide. Values are given for control, 2 weeks, and 4 weeks, for PBS and collagenase solutions. For polyureas with 0% peptide content, there is no significant change in modulus, elongation, or strength when subject to degradation in PBS or collagenase when compared with untreated samples. For polyureas with 10% peptide content, a small decrease in tensile strength and elongation

was observed at 4 weeks in collagenase, but this difference was not statistically significant. For polyureas with 20% peptide content, a statistically significant decrease in tensile strength and elongation was observed at 2 and 4 weeks. It is important to note that this difference was only present in films subjected to degradation in collagenase, not PBS alone. No statistically significant changes were seen in modulus, or in any samples in subject to degradation in PBS at 2 weeks or 4 weeks compared to untreated samples.

Percent change of modulus, elongation and strength are displayed in **Figures 3.11, 3.12, 3.13.** These results correlate well with the infrared findings that indicate cleavage of the peptide. Peptide degradation results in lower molecular weight, correlating to lower ultimate tensile strength, as discussed previously. Reduction in ultimate elongation is explicated by peptide degradation as well. Overall, the reduction in mechanical properties was attributed to peptide cleavage shown in FTIR analysis.

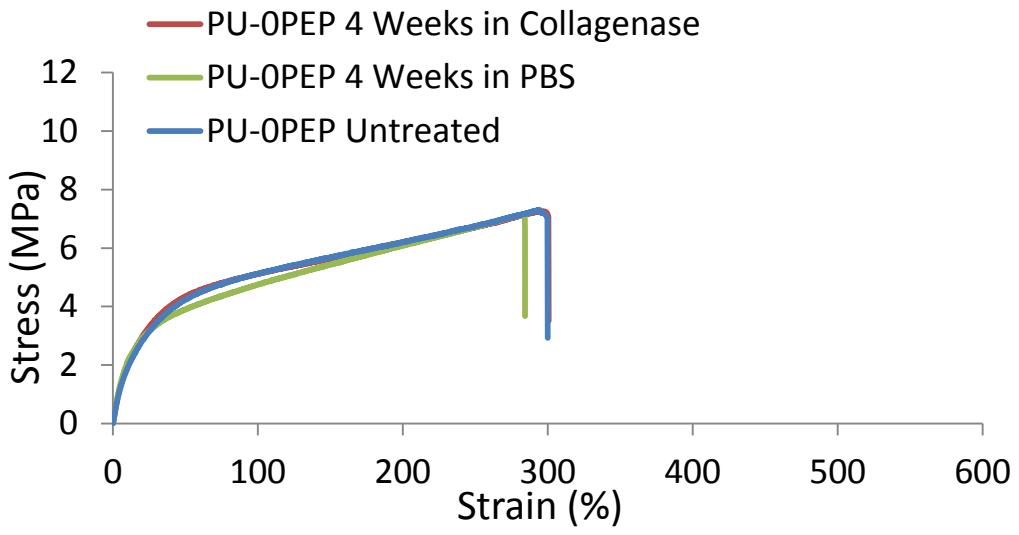

Figure 3.8 Stress-strain behavior of polyureas with 0% peptide content after 4 weeks of degradation in PBS/collagenase compared to untreated samples.

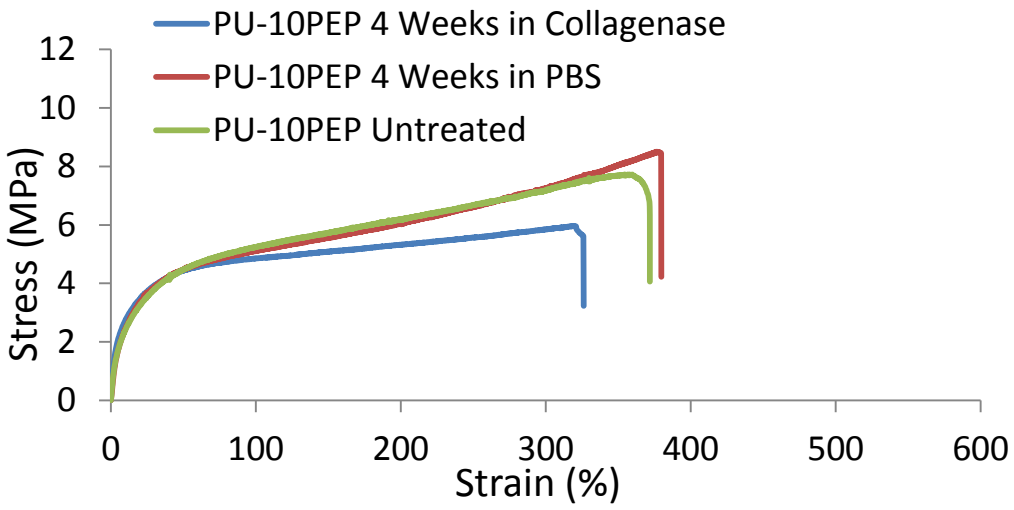

Figure 3.9 Stress-strain behavior of polyureas with 10% peptide content after 4 weeks of degradation in PBS/collagenase compared to untreated samples.

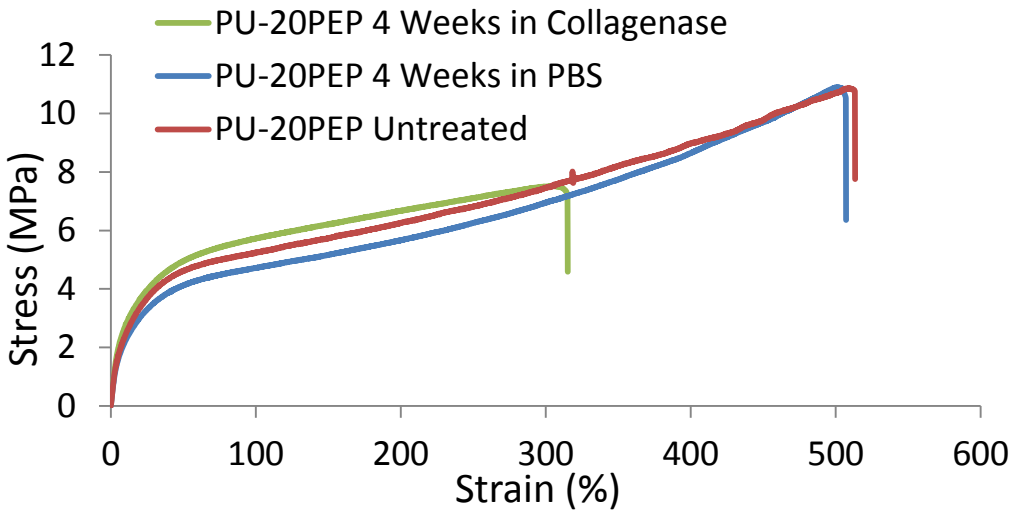

Figure 3.10 Stress-strain behavior of polyureas with 20% peptide content after 4 weeks of degradation in PBS/collagenase compared to untreated samples.

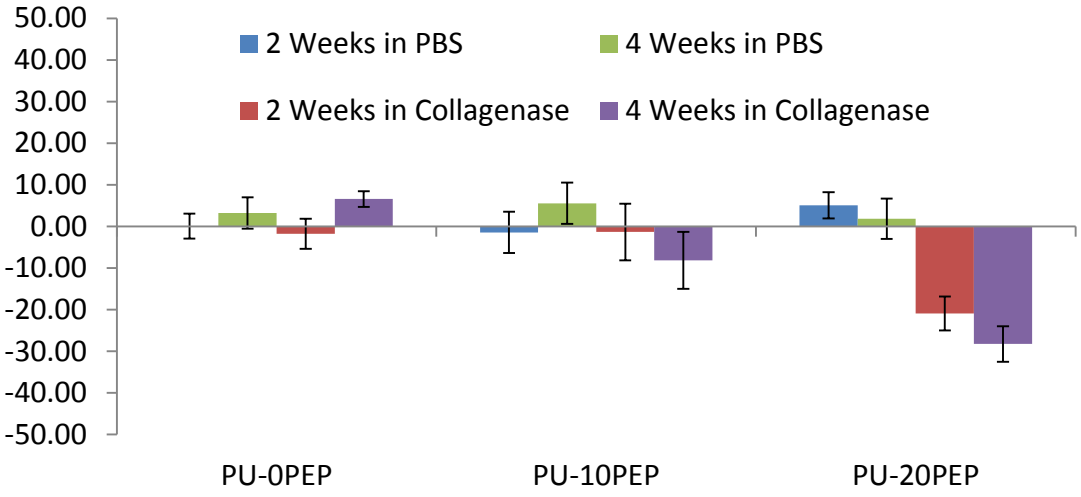

Figure 3.11 Percent change in ultimate tensile strength of specimens after 2 and 4 weeks of degradation in PBS or PBS/collagenase solution.

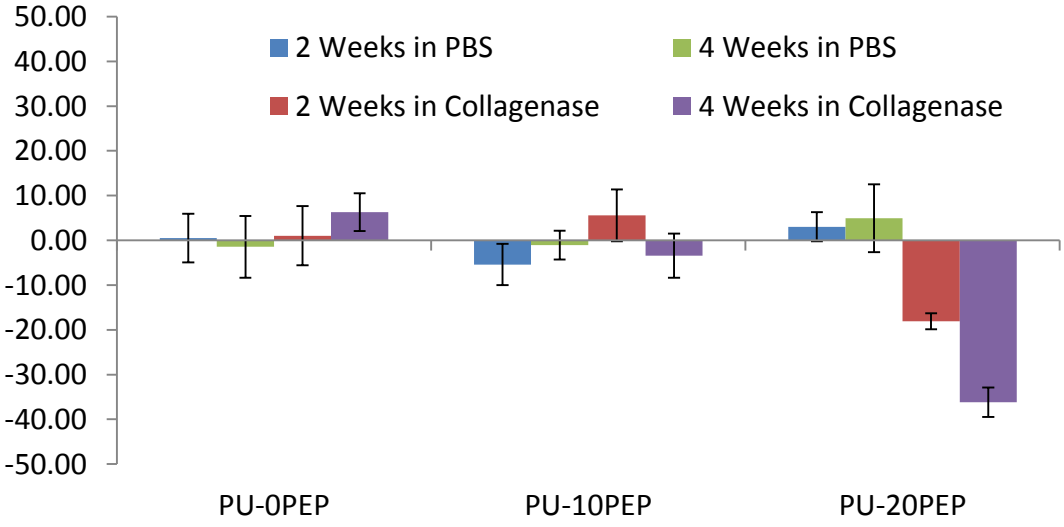

Figure 3.12 Percent change in ultimate elongation of specimens after 2 and 4 weeks of degradation in PBS or PBS/collagenase solution.

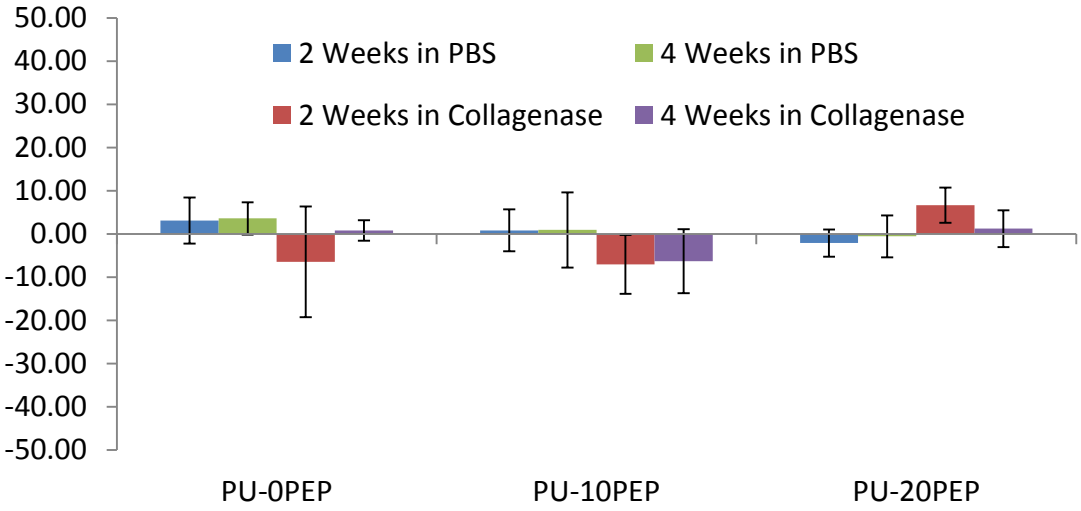

Figure 3.13 Percent change in initial (2% secant) modulus of specimens after 2 and 4 weeks of degradation in PBS or PBS/collagenase solution.

Table 3.3 Tensile properties of polyureas after 2 and 4 weeks of degradation in PBS or PBS/collagenase solution.

Modulus	**Control**	**2 weeks in PBS**	**4 weeks in PBS**	**2 weeks in Collagenase**	**4 weeks in Collagenase**
PU-0PEP	25.3 ± 0.8	26 ± 1.9	26.2 ± 1.1	23.6 ± 5.5	25.5 ± 0.4
PU-10PEP	43 ± 2.9	43.3 ± 1.3	43.4 ± 4.6	56.5 ± 5.1	57 ± 5.9
PU-20PEP	45.4 ± 1.3	44.5 ± 1.6	45.2 ± 3.1	48.5 ± 2.5	46 ± 2.6

Elongation	**Control**	**2 weeks in PBS**	**4 weeks in PBS**	**2 weeks in Collagenase**	**4 weeks in Collagenase**
PU-0PEP	310 ± 20	310 ± 10	310 ± 20	310 ± 20	330 ± 10
PU-10PEP	390 ± 10	370 ± 30	390 ± 20	360 ± 20	330 ± 20
PU-20PEP	510 ± 10	530 ± 30	540 ± 70	420 ± 10	330 ± 20

Strength	**Control**	**2 weeks in PBS**	**4 weeks in PBS**	**2 weeks in Collagenase**	**4 weeks in Collagenase**
PU-0PEP	7.2 ± 0.2	7.2 ± 0.2	7.4 ± 0.3	7 ± 0.3	7.6 ± 0.1
PU-10PEP	7.6 ± 0.4	7.5 ± 0.4	8.1 ± 0.4	6.1 ± 0.5	5.7 ± 0.2
PU-20PEP	10.8 ± 0.3	11.4 ± 0.1	11 ± 0.7	8.6 ± 0.3	7.8 ± 0.2

SEM was used to analyze the surface of degraded and control polymer films, **Figure 3.14**. Polyurea specimens with 0% peptide films were found to a very smooth topography, with no visible difference between the untreated and samples aged in collagenase for 4 weeks. The 20% peptide films were observed to have a smooth surface before degradation, but show a rough, patterned surface after being subject to degradation in collagenase solution for 4 weeks. The surface roughness is likely due to surface degradation. Enzymatic degradation is expected to be localized to the surface because enzymes are typically too large to diffuse into the polymer and cause bulk degradation.[132,216,217] The observed surface degradation is concordant with changes in chemical and tensile properties. The bond cleavage and reduction in strength support a possible reduction in molecular weight; however, due to the extent of hydrogen bonding, films could not be dissolved for molecular weight analysis with GPC. Despite the evidence of surface degradation, no significant mass loss was observed at these time points.

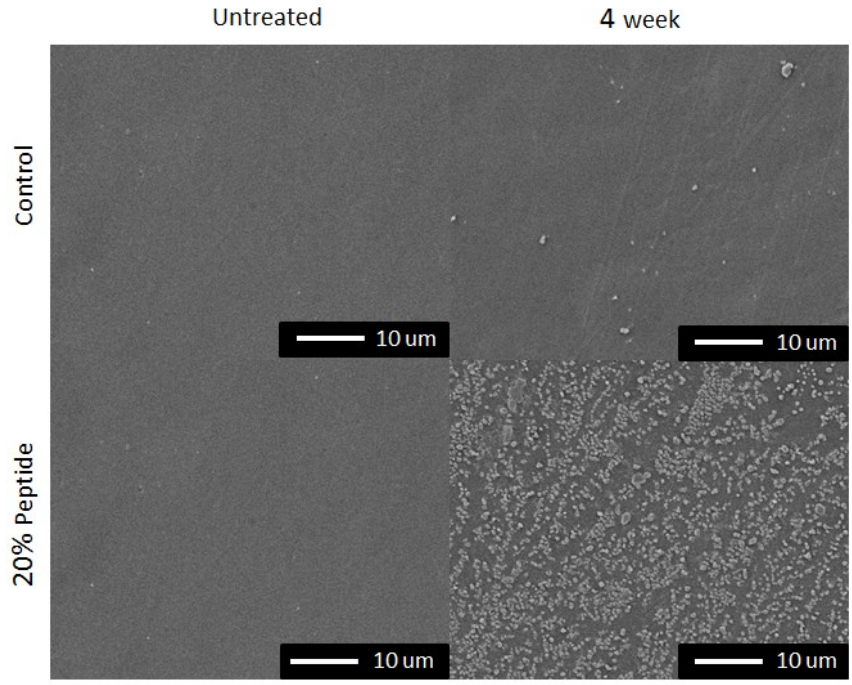

Figure 3.14 SEM images of polyurea film surface damage after 4 weeks of degradation in PBS solution with collagenase.

3.5 Conclusions

In summary, we have characterized the physical properties of a novel biodegradable polyurea and subjected it to enzymatic degradation. Infrared spectral analysis confirmed the presence of both HB urea and amide bonds in approximate proportion with their peptide content. A broadening of Tg indicative of phase mixing was observed with increased peptide content, accompanied by increased elongation and strength. This phase mixing was attributed to increased hydrogen bonding between the soft and hard segment due to the presence of amide bonds in the peptide.

FITR spectral analysis indicated a reduction in amide ($1660cm^{-1}$) bonds correlating to the enzyme-labile peptide in samples with 20% peptide content that were subjected to enzymatic degradation. This was accompanied by a statistically significant reduction in strength. These changes were not observed in specimens incubated in buffer alone or control polyureas which indicates that the observed changes were due to enzymatic degradation. In summary, the results of the current study indicate successful synthesis of polyureas with cell-responsive degradation. Further elucidation of key structure-property relationships is necessary to determine the effect of composition on microphase-separated morphology. Ultimately, understanding such relationships will be critical for the development of an improved tissue engineered ligament for ACL reconstruction.

CHAPTER IV

SUMMARY

In this study, a library of polyureas was developed to elucidate key structure property relationships for the development of a tissue engineered ligament. Polyurea formulations were optimized by investigating the effect of increased hard segment content, chain extender chemistry, and soft segment chemistry. Increases in hard segment content were shown to increase tensile modulus, elongation, and strength. However, due to the intensity of hydrogen bonding in polyureas, hard segment content could not be increased above 15% before the polymer solution would form a gel, resulting in an unprocessable polymer solution. Chain extender combinations were formulated to alter the registry of the hard segment, incrementally modifying the degree of hydrogen bonding in order to prevent gelation. Polyureas were formulated to test mixed length (EDA and BDA), mixed symmetry (EDA and 3DAP), and a combination of mixed length, symmetry, and sterically-hindering groups (2DAP and 3DAP) compared to polyureas utilizing EDA alone. Chain extenders with mixed length (EDA and BDA) and mixed symmetry (EDA and 3DAP) both successfully decreased HB urea at 1617cm^{-1} compared to polyureas made with EDA. A mixture of chain extenders with different length, symmetry, and sterically-hindering groups (2DAP and 3DAP) proved to be the most successful at reducing HB urea. Only formulations with this chain extender combination did not gel and were able to be cast into films for tensile testing.

Polyureas with PEG, PPG and PTMG soft segments were then synthesized to analyze the effect of soft segment chemistry on phase separation, chemical, and

mechanical properties. PPG polyureas were found to be mechanically weak and unsuitable for tensile load bearing applications, likely due to low molecular weight formation due to early precipitation during synthesis. PEG based polyureas had high tensile strength, but poor elasticity. It was also noted that PEG polyureas swelled in water and became mechanically weak. PTMG based polyureas had tensile strengths beyond the target value of 10 MPa and had low water uptake values. This formulation was selected for subsequent biodegradable polyurea testing.

A triblock structure for biodegradable polyureas was utilized to localize the peptide to the backbone of the soft segment. PTMG diamine was reacted with HDI to form diisocyanate functional PTMG. PTMG diisocyanate was then reacted with a shorter PEG diamine oligomer, endcapping it with PTMG, resulting in a diisocyanate functional PTMG-PEG-PTMG triblock structure. For biodegradable formulations, a portion of the PEG linker was substituted for the peptide. The optimized chain extender mixture was then added to build molecular weight. The presence of strong IR peaks assigned to hydrogen-bonded hard segments confirmed phase-separated morphology; however, overlapping of carbonyl peaks in the spectra of all peptide-based systems made quantification of peptide content difficult. Dynamic mechanical analysis confirmed a phase separated morphology and the inclusion of the peptide increased phase mixing. Tensile testing of biodegradable polyureas indicated increased elongation, strength, and initial modulus correlating to possible interaction between the hard and soft segment caused by the peptide.

Biodegradable polyurea formulations were then cast into films and subjected to degradation testing in PBS solution with and without collagenase for 4 weeks. Samples were characterized with uniaxial tensile testing and stress-strain plots were examined to determine the effects of degradation on mechanical properties. Statistically significant changes in strength and elongation of polyureas with 20% peptide content were observed for samples in collagenase solutions only. Samples subjected to degradation in PBS only saw no significant changes in mechanical properties. SEM micrographs displayed surface damage on polyureas with 20% peptide content which were subjected to degradation in collagenase. No observable change was noticed in control polyureas and biodegradable polyureas in PBS solution alone.

Overall, these polyureas combine the strength and tunability of synthetic elastomers with the cell-responsive degradation of native collagen. This hybrid design integrates the graft into native ligament remodeling and may facilitate load transfer from the biodegradable scaffold to neotissue at a rate that promotes proper tissue orientation and function while maintaining construct integrity. The addition of cell-responsive degradation to one of the most versatile classes of biomaterials makes these hybrid grafts

promising. In addition to the development of an improved biomaterial for ACL reconstruction, synthetic strategies used to generate a library of cell-responsive, biodegradable polyureas can be utilized for a variety of other biomedical applications as well. Similar to the current approach, enzyme-labile polyureas can be developed to create new structure-property models for bone or cardiovascular tissue engineering. A polymeric system that combines the tunability of segmented block copolymers with system-responsive degradation can also be used to achieve effective drug delivery.[218,219] Based on the versatility of the synthetic routes described above, enzyme-labile peptide sequences can be replaced with other sequences to produce an assortment of biomimetic materials. Overall, the synthesis of a library of cell-responsive, biodegradable polyureas will assist in the development of a tissue engineered ligament, as well as provide additional tools to advance biomaterial design.

REFERENCES

1. Albright JC, Carpenter JE, Graf BK, Richmond JC. Knee and Leg: Soft-Tissue Trauma. Rosemont, IL: American Academy of Orthopaedic Surgeons; 1999.

2. Pennisi E. Tending tender tendons. Science 2002;295(5557):1011.

3. Lyman S, Koulouvaris P, Do H, Mandl LA, Marx RG. Epidemiology of anterior cruciate ligament reconstruction: trends, readmissions, and subsequent knee surgery. J Bone Joint Surg Am 2009;91(10):2321-2328.

4. Laurencin CT, Freeman JW. Ligament tissue engineering: an evolutionary materials science approach. Biomaterials 2005;26(36):7530-7536.

5. Altman GH, Horan RL. Tissue engineering of ligaments. In: Guelcher SA, Hollinger JO, editors. An Introduction of Biomaterials. Boca Raton, FL: CRC Press; 2006. p 499-524.

6. Lin VS, Lee MC, O'Neal S, McKean J, Sung KLP. Ligament tissue engineering using synthetic biodegradable fiber scaffolds. Tissue Engineering 1999;5(5):443-451.

7. Arnoczky SP, Tarvin GB, Marshall JL. Anterior cruciate ligament replacement using patellar tendon. An evaluation of graft revascularization in the dog. The Journal of Bone and Joint Surgery 1982;64(2):217-224.

8. Lyon RM, Akeson WH, Amiel D, Kitabayashi LR, Woo SL-Y. Ultrastructural differences between the cells of the medial collateral and the anterior cruciate ligaments. Clinical Orthopaedics and Related Research 1991;272:279-286.

9. Vunjak-Novakovic G, Altman GH, Horan RL, Kaplan DL. Tissue engineering of ligaments. Annual Review of Biomedical Engineering 2004;6:131-156.

10. Nagineni CN, Amiel D, Green MH, Berchuck M, Akeson WH. Characterization of the intrinsic properties of the anterior cruciate and medial collateral ligament cells: an in vitro culture study. Journal of Orthopaedic Research 1992;10(4):465-475.

11. Yoshida M, Fujii K. Differences in cellular properties and responses to growth factors between human ACL and MCL cells. Journal of Orthopaedic Science 1999;4(4):293-298.

12. Wiig ME, Ivarsson M, Nagineni CN, Wallace CD, Arfors K-E. Type I procollagen gene expression in normal and early healing of the medial collateral and anterior cruciate ligaments in rabbits: an in situ hybridization study. Journal of Orthopaedic Research 1991;9(3):374-382.

13. Lee J, Harwood FL, Akeson WH, Amiel D. Growth factor expression in healing rabbit medial collateral and anterior cruciate ligaments. The Iowa Orthopaedic Journal 1998;18:19-25.

14. Lo IKY, Marchuk L, Hart DA, Frank CB. Comparison of mRNA levels for matrix molecules in normal and disrupted human anterior cruciate ligaments using reverse transcription-polymerase chain reaction. Journal of Orthopaedic Research 1998;16(4):421-428.

15. Guo C, Spector M. Tissue engineering of tendons and ligaments. Scaffolding in Tissue Engineering. Boca Raton, FL: Taylor & Francis; 2006. p 385-411.

16. Segawa H, Omori G, Koga Y. Long-term results of non-operative treatment of anterior cruciate ligament injury. Knee 2001;8(1):5-11.

17. Fu FH, Bennett CH, Ma CB, Menetrey J, Lattermann C. Current trends in anterior cruciate ligament reconstruction. Part II: operative procedures and clinical correlations. American Orthopaedic Society for Sports Medicine 2000;28(1):124-130.

18. Chen J, Moreau J, Horan RL, Collette A, Bramono D, Volloch V, Richmond J, Vunjak-Novakovic G, Kaplan DL, Altman GH. Ligament tissue engineering. In: Vunjak-Novakovic G, Freshney RI, editors. Culture of Cells for Tissue Engineering. Hoboken, NJ: John Wiley & Sons, Inc.; 2006. p 191-211.

19. Freeman JW, Kwansa AL. Recent advancements in ligament tissue engineering: the use of various techniques and materials for ACL repair. Recent Patents on Biomedical Engineering 2008;1(1):18-23.

20. Noyes FR, Grood ES. The strength of the anterior cruciate ligament in humans and Rhesus monkeys. Journal of Bone and Joint Surgery 1976;58A(8):1074-1082.

21. Amiel D, Kleiner JB, Roux RD, Harwood F, Akeson W. Phenomenon of ‘‘Ligamentization” : Anterior cruciate ligament reconstruction with autogenous patellar tendon. Journal of Orthopuedic Research 1986;4:162-172.

22. Fu FH, Bennett CH, Lattermann C, Ma CB. Current trends in anterior cruciate ligament reconstruction. The American Journal of Sports Medicine 1999;27(6):821-830.

23. Nedeff DD, Bach BR. Arthroscopic anterior cruciate ligament reconstruction using patellar tendon autografts. The American Journal of Knee Surgery 2001;14(4):243-257.

24. Seon JK, Song EK, Park SJ. Osteoarthritis after anterior cruciate ligament reconstruction using a patellar tendon autograft. International Orthopaedics 2006;30(2):94-98.

25. Altman GH, Horan RL. Tissue Engineering of Ligaments. In: Guelcher SA, Hollinger JO, editors. An Introduction to Biomaterials. Boca Raton, FL: CRC Press; 2006. p 499-537.

26. Kumar K, Maffulli N. The ligament augmentation device: an historical perspective arthroscopy: The Journal of Arthroscopic & Related Surgery 1999;15(4):422-432.

27. Ge Z, Goh JCH, Wang L, Tan EPS, Lee EH. Characterization of knitted polymeric scaffolds for potential use in ligament tissue engineering. Journal Biomaterial Science Polymer Edition 2005;16(9):1179-1192.

28. Friedman MJ, Sherman OH, Fox JM, Del Pizzo W, Snyder SJ, Ferkel RJ. Autogeneic anterior cruciate ligament (ACL) anterior reconstruction of the knee. Clinical Orthopaedics and Related Research 1985;196:9-14.

29. Simonian PT, Harrison SD, Cooley VJ, Escabedo EM, Deneka DA, Larson RV. Assessment of morbidity of semitendinosus and gracilis tendon harvest for ACL reconstruction. The American Journal of Knee Surgery 1997;10(2):54-59.

30. Noyes FR, Butler DL, Grood ES, Zernicke RF, Hefzy MS. Biomechanical analysis of human ligament grafts used in knee-ligament repairs and reconstructions. The Journal of Bone and Joint Surgery 1984;66(3):344-352.

31. Amiel D, Kleiner JB, Roux RD, Harwood FL, Akeson WH. The phenomenon of ‘‘ligamentization” : anterior cruciate ligament reconstruction with autogenous patellar tendon. Journal of Orthopaedic Research 1986;4:162-172.

32. Ballock RT, Woo SL-Y, Lyon RM, Hollis JM, Akeson WH. Use of patellar tendon autograft for anterior cruciate ligament reconstruction in the rabbit: a long-term histologic and biomechanical study. Journal of Orthopaedic Research 1989;7:474-485.

33. Laurencin CT, Ambrosio AMA, Borden MD, Cooper Jr. JA. Tissue engineering: orthopedic applications. Annual Review of Biomedical Engineering 1999;1:19-46.

34. Ge Z, Yang F, Goh JCH, Ramakrishna S, Lee EH. Biomaterials and scaffolds for ligament tissue engineering. Journal of Biomedical Materials Research 2006;77A:639-652.

35. Weitzel PP, Richmond JC, Altman GA, Calabro T, Kaplan DL. Future direction of the treatment of ACL ruptures. Orthopaedic Clinical North America 2002;33(4):653-661.

36. Scheffler SU, Scherler J, Pruss A, Von Versen R, Weiler A. Biomechanical comparison of human bone-patellar tendon-bone grafts after sterilization with peracetic acid ethanol. Cell and Tissue Banking 2005;6:109-115.

37. Cooper Jr. JA, Lu HH, Ko FK, Freeman JW, Laurencin CT. Fiber-based tissue-engineered scaffold for ligament replacement: design considerations and in vitro evaluation. Biomaterials 2005;26:1523-1532.

38. Lomas RJ, Jennings LM, Fisher J, Kearney JN. Effects of a peracetic acid disinfection protocol on the biocompatibility and biomechanical properties of human patellar tendon allografts. Cell and Tissue Banking 2004;5(3):149-160.

39. Shino K, Inoue M, Horibe S, Nagano J, Ono K. Maturation of allograft tendons transplanted into the knee. An arthroscopic and histological study. The Journal of Bone and Joint Surgery 1988;70-B(4):556-560.

40. Bell E. Strategy for the selection of scaffolds for tissue engineering. Tissue Engineering 1995;1:163-170.

41. Jackson DW, Lemos MJ, Tolin BS, Friedman MJ, Fu FH, Jamison J, Simon TM, McCarthy DM, Schwendeman L, Woo SL-Y. ACL reconstruction and substitutes (biologic). In: Jackson DW, editor. The Anterior Cruciate Ligament: Current and Future Concepts. New York, NY: Raven Press; 1993. p 291-356.

42. Jackson DW, Grood ES, Goldstein JD, Rosen MA, Kurzweil PA. A comparison of patellar tendon autograft and allograft used for anterior cruciate ligament reconstruction in the goat model. The American Journal of Sports Medicine 1993;21(2):176-185.

43. Jackson DW, Grood ES, Arnoczky SP, Butler DL, Simon TM. Cruciate reconstruction using freeze dried anterior cruciate ligament allograft and a ligament augmentation device (LAD). An experimental study in a goat model. The American Journal of Sports Medicine 1987;15(6):528-538.

44. Jackson DW, Windler GE, Simon TM. Intraarticular reaction associated with the use of freeze-dried, ethylene oxide-sterilized bone-patella tendon-bone allografts in the reconstruction of the anterior cruciate ligament. The American Journal of Sports Medicine 1990;18(1):1-11.

45. Jackson DW, Heinrich JT, Simon TM. Biologic and synthetic implants to replace the anterior cruciate ligament. Arthroscopy 1994;10:442-452.

46. Thomas NP, Turner IG, Jones CB. Prosthetic anterior cruciate ligaments in the rabbit: a comparison of four types of replacement. The Journal of Bone and Joint Surgery 1987;69-B(2):312-316.

47. Markolf KL, Pattee GA, Strum GM, Gallick GS, Sherman OH, Nuys V, Dorey FJ. Instrumented measurements of laxity in patients who have a Gore-Tex anterior cruciate ligament substitute. The Journal of Bone and Joint Surgery 1989;71(6):887-893.

48. Fujikawa K. In: Friedman MJ, Ferkel RD, editors. Prosthetic ligament reconstruction of the knee. Philadelphia, PA: W. B. Sanders Company; 1988. p. 1329.

49. Silver FH, Tria AJ, Zawadsky JP, Dunn MG. Anterior cruciate ligament replacement: a review. Journal of Long-Term Effects of Medical Implants 1991;1:135-154.

50. Fujikawa K. In: Friedman MJ, Ferkel RD, editors. Prosthetic Ligament Reconstruction of the Knee. Philadelphia, PA: W. B. Sanders Company; 1988.

51. Bolton CW, Bruchman WC. The Gore-Tex^{TM} expanded polytetrafluoroethylene prosthetic ligament: an in vitro and in vivo evaluation. Clinical Orthopaedics and Related Research 1985;196:202-213.

52. Richmond JC, Manseau C, Patz R, McConville O. Anterior cruciate reconstruction using a Dacron ligament prosthesis: a long-term study. The American Journal of Sports Medicine 1992;20(1):24-28.

53. Fujikawa K, Iseki F, Seedhom BB. Arthroscopy after anterior cruciate reconstruction with the Leeds-Keio ligament. The Journal of Bone and Joint Surgery 1989;71-B(4):566-570.

54. Miller RH. Knee injuries. In: Canale ST, editor. Campbell's Operative Orthopaedics. St. Louis, MO: CV Mosby; 2003. p 2274-2275.

55. McPherson GK, Mendenhall HV, Gibbons DF, Plenk H, Rottmann W, Sanford JB, Kennedy JC, Roth JH. Experimental mechanical and histologic evaluation of the Kennedy Ligament Augmentation Device. Clinical Orthopaedics and Related Research 1985;196:186-195.

56. Van Kampen CL. Biomechanics of synthetic augmentation of ligament reconstructions. Clinical Materials 1994;15:23-27.

57. Kumar K, Maffulli N. The ligament augmentation device: an historical perspective. Arthroscopy 1999;15(4):422-432.

58. Moyen BJ, Jenny JY, Mandrino AH, Lerat JL. Comparison of reconstruction of the anterior cruciate ligament with and without a Kennedy Ligament Augmentation Device. A randomized, prospective study. The Journal of Bone and Joint Surgery 1992;74:1313-1319.

59. Lopez-Vazquez E, Juan JA, Vila E, Debon J. Reconstruction of the anterior cruciate ligament with a Dacron prosthesis. The Journal of Bone and Joint Surgery 1991;73:1294-1300.

60. Murray AW, Macnicol MF. 10–16 year results of Leeds-Keio anterior cruciate ligament reconstruction. Knee 2003;11:9-14.

61. Parsons JR, Bhayani S, Alexander H, Weiss AB. Carbon fiber debris within the synovial joint. A time-dependent mechanical and histological study. Clinical Orthopaedics and Related Research 1985;196:69-76.

62. Olson EJ, Kang JD, Fu FH, Georgescu HI, Mason GC, Evans CH. The biochemical and histological effects of artificial ligament wear particles: in vitro and in vivo studies. The American Journal of Sports Medicine 1988;16:558-570.

63. Maletius W, Gillquist J. Long-term results of anterior cruciate ligament reconstruction with a Dacron prosthesis. The frequency of osteoarthritis after seven to eleven years. The American Journal of Sports Medicine 1997;25:288-293.

64. Rose FRAJ, Oreffo ROC. Bone tissue engineering: hope vs hype. Biochemical and Biophysical Research Communications 2002;292(1):1-7.

65. Kenley R, Yim K, Abrams J, Ron E, Turek T, Marden L, Hollinger J. Biotechnology and bone graft substitutes. Pharmaceutical Research 1993;10(10):1393-1401.

66. Lin VS, Lee MC, O'Neal S, McKean J, Sung K-LP. Ligament tissue engineering using synthetic biodegradable fiber scaffolds. Tissue Engineering 1999;5(5):443-451.

67. Bhatia SN, Chen CS. Tissue engineering at the micro-scale. Biomedical Microdevices 1999;2(2):131-144.

68. Neurath M. Structure and function of matrix components in the cruciate ligaments. An immunohistochemical, electron-microscopic, and immunoelectron-microscopic study. Acta Anatomica 1993;145(4):387-394.

69. Amiel D, Frank C, Harwood F, Fronek J, Akeson W. Tendons and ligaments: a morphological and biochemical comparison. Journal of Orthopaedic Research 1984;1(3):257-265.

70. Riechert K, Labs K, Lindenhayn K, Sinha P. Semiquantitative analysis of types I and III collagen from tendons and ligaments in a rabbit model. Journal of Orthopaedic Science 2001;6(1):68-74.

71. Frank CB. Ligament structure, physiology and function. Journal of Musculoskeletal and Neuronal Interactions 2004;4(2):199-201.

72. Chen EH, Black J. Materials design analysis of the prosthetic anterior cruciate ligament. Journal of Biomedical Materials Research 1980;14(5):567-586.

73. Noyes FR, Grood ES. The strength of the anterior cruciate ligament in humans and Rhesus monkeys. The Journal of Bone and Joint Surgery 1976;58A(8):1074-1082.

74. Woo SL-Y, Adams DJ. The tensile properties of human anterior cruciate ligament (ACL) and ACL graft tissues. In: Daniel D, Akeson WH, O'Connor J, editors. Knee Ligaments: Structure, Function, Injury, and Repair. New York, NY: Raven Press; 1990.

75. Woo SL-Y, Hollis JM, Adams DJ, Lyon RM, Takai S. Tensile properties of the human femur-anterior cruciate ligament-tibia complex. The effects of specimen age and orientation. The American Journal of Sports Medicine 1991;19(3):217-225.

76. Martin RB, Burr DB, Sharkey NA. Mechanical properties of ligament and tendon. Skeletal Tissue Mechanics. New York: Springer-Verlag; 1998. p 309-349.

77. Silver FH. Biomaterials, Medical Devices, and Tissue Engineering: An Integrated Approach. London, UK: Chapman & Hill; 1994. p 99-104.

78. Diamant J, Keller A, Baer E, Litt M, Arridge RG. Collagen; ultrastructure and its relation to mechanical properties as a function of ageing. Proceedings of the Royal Society of London Series B 1972;180:293-315.

79. Mosler E, Folkhard W, Knorzer E, Nemetschek-Gansler H, Nemetschek T, Koch MH. Stress-induced molecular rearrangement in tendon collagen. Journal of Molecular Biology 1985;182:589-596.

80. McBride Jr. DJ, Hahn RA, Silver FH. The morphological characterization of tendon development during chick embryogenesis: measurements of birefringence retardation. International Journal of Biological Macromolecules 1988;7:71.

81. Chvapil M, Speer D, Holubec H, Chvapil T, King D. Collagen fibers as a temporary scaffold for replacement of ACL in goats. Journal of Biomedical Materials Research 1993;27:313-325.

82. Dunn MG, Liesch JB, Tiku ML, Zawadsky JP. Development of fibroblast-seeded ligament analogs for ACL reconstruction. Journal of Biomedical Materials Research 1995;29:1363-1371.

83. Bellincampi LD, Closkey RF, Prasad R, Zawadsky JP, Dunn MG. Viability of fibroblast-seeded ligament analogs after autogenous implantation. Journal of Orthopaedic Research 1998;16(4):414-420.

84. Khor E. Methods for the treatment of collagenous tissues for bioprostheses. Biomaterials 1997;18:95-105.

85. Amiel D, Kuiper S, Newton PO, Horibe S, Woo SL-Y. Repair. Knee Ligaments: Structures, Function, Injury and Repair. New York: Raven Press; 1990. p 379-400.

86. Law JK, Parsons JR, Silver FH, Weiss AB. An evaluation of purified reconstituted type I collagen fibers. Journal of Biomedical Materials Research 1989;23(9):961-977.

87. Dunn MG, Maxian SH, Zawadsky JP. Intraosseous incorporation of composite collagen prostheses designed for ligament reconstruction. Journal of Orthopaedic Research 1994;12:128-137.

88. Dunn MG, Tria AJ, Kato YP, Bechler JR, Ochner RS, Zawadsky JP, Silver FH. Anterior cruciate ligament reconstruction using a composite collagenous prosthesis. A biomechanical and histologic study in rabbits. The American Journal of Sports Medicine 1992;20:507-515.

89. Dunn MG, Bellincampi LD, Tria AJ, Zawadsky JP. Preliminary development of a collagen-PLA composite for ACL reconstruction. Journal of Applied Polymer Science 1997;63:1423-1428.

90. Koob TJ, Hernandez DJ. Material properties of polymerized NDGA-collagen composite fibers: development of biologically based tendon constructs. Biomaterials 2002;23(1):203-212.

91. Caruso AB, Dunn MG. Functional evaluation of collagen fiber scaffolds for ACL reconstruction: Cyclic loading in proteolytic enzyme solutions. Journal of Biomedical Materials Research 2004;69A(1):164-171.

92. Lee CH, Singla A, Lee Y. Biomedical applications of collagen. International Journal of Pharmaceutics 2001;221(1-2):1-22.

93. Fan H, Liu H, Toh SL, Goh JCH. Enhanced differentiation of mesenchymal stem cells co-cultured with ligament fibroblasts on gelatin/silk fibroin hybird scaffold. Biomaterials 2008;29:1017-1027.

94. Liu H, Ge Z, Wang Y, Toh SL, Sutthikhum V, Goh JCH. Modification of sericin-free silk fibers for ligament tissue engineering application. Journal of Biomedical Materials Research, Part B: Applied Biomaterials 2007;82(1):129-138.

95. Toh SL, Teh TKH, Vallaya S, Goh JCH. Novel silk scaffolds for ligament tissue engineering applications. Key Engineering Materials 2006;326-328:727-730.

96. Altman GH, Diaz F, Jakuba C, Calabro T, Horan RL, Chen J, Lu H, Richmond J, Kaplan DL. Silk-based biomaterials. Biomaterials 2003;24:401-416.

97. Chen X, Qi Y-Y, Wang L-L, Yin Z, Yin G-L, Zou X-H, Ouyang H-W. Ligament regeneration using a knitted silk scaffold combined with collagen matrix. Biomaterials 2008;29:3683-3692.

98. Altman GH, Horan RL, Lu HH, Moreau J, Martin I, Richmond J, Kaplan DL. Silk matrix for tissue engineered anterior cruciate ligaments. Biomaterials 2002;23(20):4131-4141.

99. Chen J, Altman GH, Karageorgiou V, Horan RL, Collette A, Volloch V, Colabro T, Kaplan DL. Human bone marrow stromal cell and ligament fibroblast response on RGD-modified silk fibers. Journal of Biomedical Materials Research 2003;67A(2):559-570.

100. Funakoshi T, Majima T, Iwasaki N, Yamane S, Masuko T, Minami A, Harada K, Tamura H, Tokura S, Nishimura S-I. Novel chitosan-based hyaluronan hybrid polymer fibers as a scaffold in ligament tissue engineering. Journal of Biomedical Materials Research 2005;74A:338-346.

101. Messenger MP, Raif EM, Seedhom B, Brookes SJ. The potential use of enamel matrix derivative for in situ anterior cruciate ligament tissue engineering: a translational in vitro investigation. Tissue Engineering 2007;13:2041-2051.

102. Bourke SL, Kohn J, Dunn MG. Preliminary development of a novel resorbable synthetic polymer fiber scaffold for anterior cruciate ligament reconstruction. Tissue Engineering 2004;10:43-52.

103. Buma P, Kok HJ, Blankevoort L, Kuijpers W, Huiskes R, Van Kampen A. Augmentation in anterior cruciate ligament reconstruction-a histological and biomechanical study on goats. International Orthopaedics 2004;28:91-96.

104. Ge Z, Goh JCH, Wang L, Tan EPS, Lee EH. Characterization of knitted polymeric scaffolds for potential use in ligament tissue engineering. Journal of Biomaterials Science, Polymer Edition 2005;16(9):1179-1192.

105. Laitinen O, Alitalo I, Toivonen T, Vasenius J, Tormala P, Vainionpaa S. Tissue response to a braided poly-L-lactide implant in an experimental reconstruction of anterior cruciate ligament. Journal of Materials Science: Materials in Medicine 1993;4:547-554.

106. Sahoo S, Goh JCH, Toh SL. Development of hybrid polymer scaffolds for potential applications in ligament and tendon tissue engineering. Biomedical Materials 2007;2:167-173.

107. Sahoo S, Ouyang H, Goh JCH, Tay TE, Toh SL. Characterization of a novel polymeric scaffold for potential application in tendon/ligament tissue engineering. Tissue Engineering 2006;12:91-99.

108. Shao H-J, Chen CS, Lee I-C, Wang J-H, Young T-H. Designing a three-dimensional expanded polytetrafluoroethylene–poly(lactic-co-glycolic acid) scaffold for tissue engineering. Artificial Organs 2009;33(4):309-317.

109. Lu HH, Cooper Jr. JA, Manuel S, Freeman JW, Attawia MA, Ko FK, Laurencin CT. Anterior cruciate ligament regeneration using braided biodegradable scaffolds: in vitro optimization studies. Biomaterials 2005;26:4805-4816.

110. Freeman JW, Woods MD, Laurencin CT. Tissue engineering of the anterior cruciate ligament using a braid-twist scaffold design. Journal of Biomechanics 2007;40:2029-2036.

111. Park TG. Degradation of poly(lactic-co-glycolic acid) microspheres: effect of copolymer composition. Biomaterials 1995;16(15):1123-1130.

112. Lamba NMK, Woodhouse KA, Cooper SL. Polyurethanes in Biomedical Applications. Boca Raton, FL: CRC Press LLC; 1998.

113. Gogolewski S. Selected topics in biomedical polyurethanes. A review. Colloid & Polymer Science 1989;267(9):757-785.

114. Guelcher SA. Biodegradable polyurethanes: synthesis and applications in regenerative medicine. Tissue Engineering, Part B: Reviews 2008;14(1):3-17.

115. Santerre JP, Woodhouse KA, Laroche G, Labow RS. Understanding the biodegradation of polyurethanes: From classical implants to tissue engineering materials. Biomaterials 2005;26(35):7457-7470.

116. The Polyurethanes Book. New York, NY: John Wiley & Sons, Ltd.; 2002. p 1-8.

117. Oertel G. Polyurethane Handbook. Berlin, Germany: Hanser Gardner Publications, Inc.; 1994.

118. Stokes K, McVenes R. Polyurethane elastomer biostability. Journal of Biomaterials Applications 1995;9(4):321-354.

119. Szycher M, Reed A. Biostable polyurethane elastomers. Medical Device Technology 1992;3(10):42–51.

120. Lelah MD, Cooper SL. Polyurethanes in Medicine. Boca Raton, FL: CRC Press, Inc.; 1986.

121. Szycher M. Szycher's Handbook of Polyurethanes. Boca Raton, FL: CRC Press, Inc.; 1999.

122. Gogolewski S. In vitro and in vivo molecular stability of medical polyurethanes: a review. Trends in Polymer Science 1991;1(1):47-61.

123. Legge N, Helden G, Schoeder H. Thermoplastic Elastomers: A Comprehensive Review. New York, NY: Macmillan Publishing Company; 1987.

124. Bonart R, Morbitzer L, Hentze G. X-ray investigations concerning the physical structure of cross-linking in urethane elastomers. II. Butanediols as chain extender. Journal of Macromolecular Science, Part B 1969;3(2):337-356.

125. Bonart R, Morbitzer L, Muller EH. X-ray investigations concerning the physical structure of crosslinking in urethane elastomers. III. Common structure principles for extensions with aliphatic diamines and diols. Journal of Macromolecular Science, Part B 1974;9(3):447-461.

126. Christenson EM, Anderson JM, Hiltner A, Baer E. Relationship between nanoscale deformation processes and elastic behavior of polyurethane elastomers. Polymer 2005;46(25):11744-11754.

127. Martin DJ, Meijs GF, Gunatillake PA, Yozghatlian SP, Renwick GM. The influence of composition ratio on the morphology of biomedical polyurethanes. Journal of Applied Polymer Science 1999;71(6):937-952.

128. Santerre J, Labow R. The effect of hard segment size on the hydrolytic stability of polyether-urea-urethanes when exposed to cholesterol esterase. Journal of Biomedical Materials Research 1997;36(2):223-232.

129. Chang Y-JP, Wilkes GL. Superstructure in segmented polyether-urethanes. Journal of Polymer Science, Part B. Polymer Physics 1975;13(3):455-476.

130. Zha L, Wu M, Yang J. Hydrogen bonding and morphological structure of segmented polyurethanes based on hydroquinone–bis(b-hydroxyethy)ether as a chain extender. Journal of Applied Polymer Science 1999;73(14):2895-2902.

131. O'Sickey MJ, Lawrey BD, Wilkes GL. Structure–property relationships of poly(urethane urea)s with ultra-low monol content poly(propylene glycol) soft segments. I. Influence of soft segment molecular weight and hard segment content. Journal of Applied Polymer Science 2002;84(2):229-243.

132. Skarja GA, Woodhouse KA. Structure-property relationships of degradable polyurethane elastomers containing an amino acid-based chain extender. Journal of Applied Polymer Science 2000;75(12):1522-1534.

133. Gisselfalt K, Helgee B. Effect of soft segment length and chain extender structure on phase separation and morphology in poly(urethane urea)s. Macromolecular Materials and Engineering 2003;288:265-271.

134. Gisselfalt K, Edberg B, Flodin P. Synthesis and properties of degradable poly(urethane urea)s to be used for ligament reconstructions. Biomacromolecules 2002;3(5):951-958.

135. Coury A. Chemical and biochemical degradation of polymers. In: Ratner B, Hoffman A, Schoen F, Lemons J, editors. Biomaterials Science: An Introduction to Materials in Medicine. Boston, MA: Elsevier Academic Press; 2004. p 411-430.

136. Mazzu AL, Smith CP. Determination of extractable methylene dianiline in thermoplastic polyurethanes by HPLC. Journal of Biomedical Materials Research 1984;18(8):961-968.

137. Szycher M, Siciliano AA. An assessment of 2,4 TDA formation from Surgitek polyurethane foam under simulated physiological conditions. Journal of Biomaterials Applications 1991;5(4):323-336.

138. Guelcher S, Srinivasan A, Hafeman A, Gallagher KM, Doctor JS, Khetan S, Mcbride S, Hollinger JO. Synthesis, in vitro degradation, and mechanical properties of two-component poly(ester urethane) urea scaffolds: effects of water and polyol composition. Tissue Engineering 2007;13(9):2321-2333.

139. Saad B, Ciardelli G, Matter S, Welti M, Uhlschmid GK, Neuenschwander P, Suter U. Degradable and highly porous polyestherurethane foam as biomaterials: effects and phagocytosis of degradation products in osteoblasts. Journal of Biomedical Materials Research 1998;39(4):594-602.

140. Saad B, Hirt TD, Welti M, Uhlschmid GK, Neuenschwander P, Suter UW. Development of degradable polyesterurethanes for medical applications: In vitro and in vivo evaluations. Journal of Biomedical Materials Research 1997;36(1):65-74.

141. Saad B, Kuboki M, Matter S, Welti M, Uhlschmid GK, Neuenschwander P, Suter U. DegraPol-foam: a degradable and highly porous polyesterurethane as a new substrate for bone formation. Artificial Organs 2000;24(12):939-945.

142. Skarja GA, Woodhouse KA. Synthesis and characterization of degradable polyurethane elastomers containing an amino acid-based chain extender. Journal of Biomaterials Science, Polymer Edition 1998;9(3):271-295.

143. Skarja GA, Woodhouse KA. In vitro degradation and erosion of degradable, segmented polyurethanes containing an amino acid-based chain extender. Journal of Biomaterials Science, Polymer Edition 2001;12(8):851-873.

144. Zhang J, Beckman E, Piesco P, Agarwal A. A new peptide-based urethane polymer: synthesis, biodegradation, and potential to support cell growth in vitro. Biomaterials 2000;21:1247-1258.

145. Zhang JY, Beckman EJ, Hu J, Yang GG, Agarwal S, Hollinger JO. Synthesis, biodegradability, and biocompatibility of lysine diisocyanate-glucose polymers. Tissue Engineering 2002;8(5):771-785.

146. Zhang JY, Doll BA, Beckman EJ, Hollinger JO. A biodegradable polyurethane-ascorbic acid scaffold for bone tissue engineering. Journal of Biomedical Materials Research 2003;67A(2):389-400.

147. Guelcher S, Wilkes G. Synthesis of biocompatible segmented polyurethanes from aliphatic diisocyanates and diurea diol chain extenders. Acta Biomaterialia 2005;1(4):471-484.

148. Guelcher SA, Patel V, Gallagher KM, Connolly S, Didier JE, Doctor JS, Hollinger JO. Synthesis and in vitro biocompatibility of injectable polyurethane foam scaffolds. Tissue Engineering 2006;12(5):1247-1259.

149. Bruin P, Veenstra GJ, Nijenhuis AJ, Pennings AJ. Design and synthesis of biodegradable poly(ester-urethane) elastomer networks composed of non-toxic building blocks. Makromolekulare Chemie, Rapid Communcations 1988;9(8):589-594.

150. Gorna K, Gogolewski S. Biodegradable polyurethane implants: II. in vitro degradation and calcification of materials from poly (e-caprolactone)-poly(ethylene oxide) diols and various chain extenders. Journal of Biomedical Materials Research 2002;60(4):592-606.

151. Guan J, Sacks MS, Beckman EJ, Wagner WR. Synthesis, characterization, and cytocompatibility of polyurethaneurea elastomers with designed elastase sensitivity. Biomacromolecules 2005;6(5):2833-2842.

152. Asplund BJO, Bowden T, Mathisen T, Hilborn J. Synthesis of highly elastic biodegradable poly(urethane urea). Biomacromolecules 2007;8(3):905-911.

153. Gogolewski S, Gorna K. Biodegradable polyurethane cancellous bone graft substitutes in the treatment of iliac crest defects. Journal of Biomedical Materials Research 2007;80A(1):94–101.

154. Gogolewski S, Gorna K, Turner AS. Regeneration of bicortical defects in the iliac crest of estrogen-deficient sheep, using new biodegradable polyurethane bone graft substitutes. Journal of Biomedical Materials Research 2006;77A(4):802–810.

155. Elliott SL, Fromstein JD, Santerre JP, Woodhouse KA. Identification of biodegradation products formed by L-phenylalanine based segmented polyurethaneureas. Journal of Biomaterials Science, Polymer Edition 2002;13(6):691–711.

156. Cohn D, Stern T, Gonzales M, Epstein J. Biodegradable poly(ethylene oxide)/poly(e-caprolactone) multiblock copolymers. Journal of Biomedical Materials Research 2002;59(2):273-281.

157. Woo GLY, Mittelman MW, Santerre JP. Synthesis and characterization of a novel biodegradable antimicrobial polymer. Biomaterials 2000;21(12):1235-1246.

158. Borkenhagen M, Stoll RC, Neuenschwander P, Suter UW, Aebischerl P. In vivo performance of a new biodegradable polyester urethane system used as a nerve guidance channel. Biomaterials 1998;19(23):2155-2165.

159. Guan J, Sacks M, Beckman E, Wagner W. Biodegradable poly(ether ester urethane urea) triblock copolymers and purtrescine: synthesis, characterisation and cytocompatibility. Biomaterials 2004;25(1):85-96.

160. Cohn D, Hotovely-Salomon A. Biodegradable multiblock PEO/PLA thermoplastic elastomers: molecular design and properties. Polymer 2005;46(7):2068-2075.

161. Storey RF, Wiggins JS, Mauritz KA, Puckett AD. Bioabsorbable composites: II. nontoxic, L-lysine based poly(ester urethane) matrix composites. Polymer Composites 1993;14(1):17-25.

162. Storey RF, Wiggins JS, Puckett AD. Hydrolyzable poly(ester-urethane) networks from L-lysine diisocyanate and D,L-lactide/e-caprolactone homo- and copolyester triols. Journal of Polymer Science 1994;32(12):2345-2363.

163. Liljensten E, Gisselfalt K, Edberg B, Bertilsson H, Flodin P. Studies of polyurethane urea bands for ACL reconstruction. Journal of Materials Science: Materials in Medicine 2002;13:351-359.

164. Gorna K, Gogolewski S. Preparation, degradation, and calcification of biodegradable polyurethane foams for bone graft substitutes. Journal of Biomedical Materials Research 2003;67A(3):813–827.

165. Sawhney AS, Hubbell JA. Rapidly degraded terpolymers of dl-lactide, glycolide, and ε-caprolactone with increased hydrophilicity by copolymerization with polyethers. Journal of Biomedical Materials Research 1990;24:1397-1411.

166. Fromstein JD, Woodhouse KA. Elastomeric biodegradable polyurethane blends for soft tissue applications. Journal of Biomaterials Science, Polymer Edition 2002;13(4):391-406.

167. Abousleiman RI, Sikavitsas VI. Bioreactors for tissues of the musculoskeletal system. Advances in Experimental Medicine and Biology 2006;585:243-259.

168. Park SA, Kim IA, Lee YJ, Shin JW, Kim C-R, Kim JK, Yang Y-I, Shin J-W. Biological responses of ligament fibroblasts and gene expression profiling on micropatterned silicone substrates subjected to mechanical stimuli Journal of Bioscience and Bioengineering 2006;102(5):402-412.

169. Zeichen J, van Griensven M, Bosch U. The proliferative response of isolated human tendon fibroblasts to cyclic biaxial mechanical strain. The American Journal of Sports Medicine 2000;28(6):888-892.

170. Yang G, Crawford RC, Wang JH-C. Proliferation and collagen production of human patellar tendon fibroblasts in response to cyclic uniaxial stretching in serum-free conditions. Journal of Biomechanics 2004;37(10):1543-1550.

171. Almekinders LC, Banes AJ, Bracey LW. An in vitro investigation into the effects of repetitive motion and nonsteroidal antiinflammatory medication on human tendon fibroblasts. The American Journal of Sports Medicine 1995;23(1):119-123.

172. Miyaki S, Ushida T, Nemoto K, Shimojo H, Itabashi A, Ochiai N, Miyanaga Y, Tateishi T. Mechanical stretch in anterior cruciate ligament derived cells regulates type I collagen and decorin expression through extracellular signal-regulated kinase 1/2 pathway. Materials Science and Engineering 2001;17(1-2):91-94.

173. Lee CH, Shin HJ, Cho IH, Kang Y-M, Kim IA, Park K-D, Shin J-W. Nanofiber alignment and direction of mechanical strain affect the ECM production of human ACL fibroblast. Biomaterials 2005;26(11):1261-1270.

174. Toyoda T, Matsumoto H, Fujikawa K, Saito S, Inoue K. Tensile load and the metabolism of anterior cruciate ligament cells. Clinical Orthopaedics and Related Research 1998(353):247-255.

175. Hannafin JA, Attia EA, Henshaw R, Warren RF, Bhargava MM. Effect of cyclic strain and plating matrix on cell proliferation and integrin expression by ligament fibroblasts. Journal of Orthopaedic Research 2006;24(2):149-158.

176. Henshaw DR, Attia E, Bhargava M, Hannafin JA. Canine ACL fibroblast integrin expression and cell alignment in response to cyclic tensile strain in three-dimensional collagen gels. Journal of Orthopaedic Research 2006;24(3):481-490.

177. Gilbert TW, Stewart-Akers AM, Sydeski J, Nguyen TD, Badylak SF, Woo SL-Y. Gene expression by fibroblasts seeded on small intestinal submucosa and subjected to cyclic stretching. Tissue Engineering 2007;13(6):1313-1323.

178. Wang JH-C, Jia F, Gilbert TW, Woo SL-Y. Cell orientation determines the alignment of cell-produced collagenous matrix. Journal of Biomechanics 2003;36(1):97-102.

179. Wang JH-C, Yang G, Li Z, Shen W. Fibroblast responses to cyclic mechanical stretching depend on cell orientation to the stretching direction. Biomaterials 2004;37(4):573-576.

180. Jones BF, Banes AJ, Wall ME, Carroll RL, Washburn S. Ligament cells stretched on a microgrooved substrate increase intracellular calcium in response to a mechanical stimulus. Materials Research Society symposia proceedings 2004;EXS(1):197.

181. Jones BF, Wall ME, Carroll RL, Washburn S, Banes AJ. Ligament cells stretch-adapted on a microgrooved substrate increase intercellular communication in response to a mechanical stimulus. Journal of Biomechanics 2005;38(8):1653-1664.

182. Kim S-G, Akaike T, Sasagawa T, Atomi Y, Kurosawa H. Gene expression of type I and type III collagen by mechanical stretch in anterior cruciate ligament cells. Cell Structure and Function 2002;27(3):139-144.

183. Hsieh AH, Tsai CM-H, Ma Q-J, Lin T, Banes AJ, Villareal FJ, Akeson WH, Sung K-LP. Time-dependent increases in type-III collagen gene expression in medial collateral ligament fibroblasts under cyclic strains. Journal of Orthopaedic Research 2000;18(2):220-227.

184. Lee C-Y, Liu X, Smith CL, Zhang X, Hsu H-C, Wang D-Y, Luo Z-P. The combined regulation of estrogen and cyclic tension on fibroblast biosynthesis derived from anterior cruciate ligament. Matrix Biology 2004;23(5):323-329.

185. Foos MJ, Hickox JR, Mansour PG, Slauterbeck JR, Hardy DM. Expression of matrix metalloprotease and tissue inhibitor of metalloprotease genes in human anterior cruciate ligament. Journal of Orthopaedic Research 2001;19(4):642-649.

186. Zhou D, Lee HS, Villareal F, Teng A, Lu E, Reynolds S, Qin C, Smith J, Sung KLP. Differential MMP-2 activity of ligament cells under mechanical stretch injury: an in vitro study on human ACL and MCL fibroblasts. Journal of Orthopaedic Research 2005;23(4):949-957.

187. Kerkvliet EHM, Docherty AJP, Beersten W, Everts V. Collagen breakdown in soft connective tissue explants is associated with the level of active gelatinase A (MMP-2) but not with collagenase Matrix Biology 1999;18(4):373-380.

188. Bramono DS, Richmond JC, Weitzel PP, Chernoff H, Martin I, Volloch V, Jakuba CM, Diaz F, Gandhi JS, Kaplan DL and others. Characterization of transcript levels for matrix molecules and proteases in ruptured human anterior cruciate ligaments. Connective Tissue Research 2005;46(1):53-65.

189. Sottrup-Jensen L, Birkedal-Hansen H. Human fibroblast collagenase-alpha-macroglobulin interactions. Localization of cleavage sites in the bait regions of five mammalian alpha-macroglobulins. Journal of Biological Chemistry 1989;264(1):393-401.

190. Welgus HG, Jefferey JJ, Eisen AZ. The collagen substrate specificity of human skin fibroblast collagenase. Journal of Biological Chemistry 1981;256(18):9511-9515.

191. Whitham SE, Murphy G, Angel P, Rahmsdorf HJ, Smith B, Lyons A, Harris RJR, Reynolds JJ, Herrlich P, Docherty AJ. Comparison of human stromelysin and collagenase by cloning and sequence analysis. Biochemical Journal 1986;240(3):913-916.

192. Primeaux D, Zimmerman R, Hillman K; Method of preparing spray elastomer systems. patent 6605684. 2003.

193. Roesler R, Squiller E; Polyurea coatings from dimethyl-substituted polyaspartic mixtures patent. 6482333. 2002.

194. Raju KVSN, Chattopadhyay DK. Structural engineering of polyurethane coatings for high performance applications. Prog. Polym. Sci. 2006;32:352-418.

195. Miller J, Lin S, Hwang K, Wu K, Gibson P, Cooper S. Properties of polyether-polyurethane block copolymers: effects of hard segment length distribution. Macromolecules 1985;18:32-44.

196. Paik Sung CS, Hu CB, Wu CS. Properties of aegmented poly(urethaneureas) based on 2,4-toluene diisocyanate. 1. Thermal transitions, X-ray studies, and comparison with segmented poly(urethanes). Macromolecules 1980;13(1):111-116.

197. Adhikari R, Gunatillake PA, McCarthy SJ, Meijs GF. Mixed macrodiol-based siloxane polyurethanes: Effect of the comacrodiol structure on properties and morphology. Journal of Applied Polymer Science 2000;78(5):1071-1082.

198. Martin DJ, Meijs GF, Gunatillake PA, McCarthy SJ, Renwick GM. The effect of average soft segment length on morphology and properties of a series of polyurethane elastomers. II. SAXS-DSC annealing study. Journal of Applied Polymer Science 1997;64(4):803-817.

199. Wang CB, Cooper SL. Morphology and properties of segmented polyether polyurethaneureas. Macromolecules 1983;16(5):775-786.

200. Iriuchishima T, Yorifuji H, Aizawa S, Tajika Y, Murakami T, Fu FH. Evaluation of ACL mid-substance cross-sectional area for reconstructed autograft selection. Knee Surg Sports Traumatol Arthrosc 2014;22(1):207-13.

201. Shelburne K, Pandy M, Anderson F, Torry M. Pattern of anterior cruciate ligament force in normal walking. Journal of Biomechanics 2004;37:797-805.

202. Wicks D, Yeske P. Control of the Reactions between Polyaspartic Esters and Alipathic Polyisocyanates. 1993; New Orleans, LA.

203. Wicks D, Yeske P; Polyurea coating compositionshaving improved pot lives patent US5243012 A. 1993.

204. Rathi S, Chen X, Coughlin EB, Hsu SL, Golub CS, Tzivanis MJ. Toughening semicrystalline poly(lactic acid) by morphology alteration. Polymer 2011;52(19):4184-4188.

205. Sarkar D, Yang J-C, Lopina S. Structure-property relationship of L-tyrosine-based polyurethanes for biomaterial applications. Journal of Applied Polymer Science 2008;108(4):2345-2355.

206. Smith TL. Strength of elastorners—a perspective. Polymer Engineering & Science 1977;17(3):129-143.

207. Spaans C, de Groot J, Dekens F, Pennings A. High molecular weight polyurethanes and a polyurethane urea based on 1,4-butanediisocyanate. Polymer Bulletin 1998;41:131-138.

208. Han J, Chen B, Ye L, Zhang A-Y, Zhang J, Feng Z-G. Synthesis and characterization of biodegradable polyurethane based on poly(ε-caprolactone) and L-lysine ethyl ester diisocyanate. Frontiers of Materials Science in China 2009;3(1):25-32.

209. Dillon J. Infared spectroscopic atlas of polyurethanes. Lancaster, PA: Technomic Publication 1989.

210. Speckhard TA, Cooper SL. Ultimate tensile properties of segmented polyurethane elastomers: Factors leading to reduced properties for polyurethanes based on nonpolar soft segments. Rubber Chemistry and Technology 1986;59(3):405-431.

211. Li C, Yu X, Speckhard TA, Cooper SL. Synthesis and properties of poly(cyanoethylmethylsiloxane) polyurea urethane elastomers: a study of segmental compatibility. Journal of Polymer Science, Part B: Polymer Physics 1988;26(2):315-317.

212. Miller D, Forrester K, Hart DA, Leonard C, Salo P, Bray RC. Endothelial dysfunction and decreased vascular responsiveness in the anterior cruciate ligament-deficient model of osteoarthritis. The Journal of Applied Physiology 2007;102(3):1161-1169.

213. Berger SE, Szukiewicz W. High-performance toluene diisocyanate-polypropylene glycol castable elastoplastics. I&EC Product Research and Development 1964;3(2):129-132.

214. Rizzi SC, Hubbell JA. Recombinant protein-co-PEG networks as cell-adhesive and proteolytically degradable hydrogel matrixes. Part I: Development and physicochemical characteristics. Biomacromolecules 2005;6(3):1226-1238.

215. Mann B, Gobin A, Tsai A, Schmedlen R, West J. Smooth muscle cell growth in photopolymerized hydrogels with cell adhesive and proteolytically degradable domains: synthetic ECM analogs for tissue engineering. Biomaterials 2001;22:3045-3051.

216. Lyu S, Untereker D. Degradability of polymers for implantable biomedical devices. International Journal of Molecular Sciences 2009;10(9):4033-4065.

217. Burkersroda F, Schedl L, Göpferich A. Why degradable polymers undergo surface erosion or bulk erosion. Biomaterials 2002;23:4221-4231.

218. Balmayor ER, Tuzlakoglu K, Marques AP, Azevedo HS, Reis RL. A novel enzymatically-mediated drug delivery carrier for bone tissue engineering applications: combining biodegradable starch-based microparticles and differentiation agents. Journal of Materials Science: Materials in Medicine 2008;19:1617-1623.

219. Vemula PK, Cruikshank GA, Karp JM, John G. Self-assembled prodrugs: An enzymatically triggered drug-delivery platform. Biomaterials 2009;30:383-393.